Sensing of Citrulline Modifications in Histone Peptides by Deep Cavitand Hosts

*Adam D. Gill,[b] Briana L. Hickey,[a] Siwen Wang,[c] Min Xue,[a,c] Wenwan Zhong[a,c] and Richard J. Hooley[a,b]**

[a]Department of Chemistry; [b]Department of Biochemistry and Molecular Biology; [c]Environmental Toxicology Program; University of California-Riverside, Riverside, CA, 92521, U.S.A.

richard.hooley@ucr.edu

Electronic Supplementary Information

Table of Contents

1. General Information.

Cavitand **1**[1] and guest **G1**[2] were synthesized and characterized according to literature procedures. For detailed analysis of the fluorescence response of guests **G1**[2] and **G2**[3,4] in host **1**, please see the cited references. Trans-[4-(dimethylamino)styryl]-1-methylpyridinium iodide (DSMI) **G2** was purchased from Sigma Aldrich (St. Louis, MO). All other materials were purchased from Sigma Aldrich (St. Louis, MO) or Fisher Scientific (Fairlawn, NJ), and were used as received. NMR spectra were recorded on a Bruker Avance Neo 400 MHz or 600 MHz NMR spectrometer. All NMR spectra were processed using MestReNova by Mestrelab. Research S.L. Deuterated NMR solvents were obtained from Cambridge Isotope Laboratories, Inc., Andover, MA, and used without further purification. Molecular modelling (Hartree-Fock) was performed using SPARTAN '06. Fluorescence measurements were performed in either a Bio-Tek Synergy HT Multi-Detection Microplate Reader, or a Perkin Elmer Wallac 1420 Victor 2 Microplate Reader (PerkinElmer), with the Ex/Em wavelengths at 530/605 nm or 485/605 nm.

2. New Molecule Synthesis and Characterization

Amide Cavitand 2:

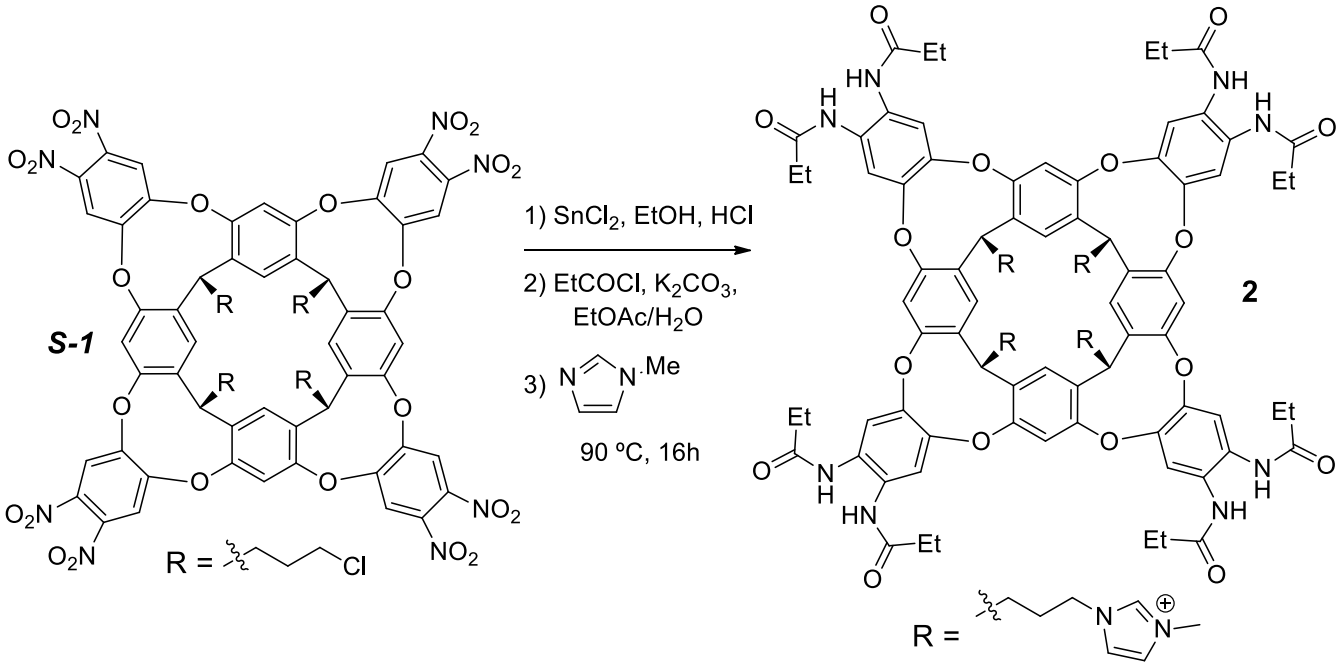

Chloro-amide cavitand. Cavitand **2** was synthesized via an adaptation of Rebek's literature procedure.[5] Chloro-nitro cavitand ***S-1*** (100 mg, 0.16 mmol) was placed in a round-bottomed flask with excess tin (II) chloride dihydrate (450 mg) and a stir bar. A 4:1 mixture of ethanol and concentrated HCl (4:1 mL) was added to the flask and the reaction was stirred at 75° C overnight. The reaction mixture was cooled, and the solvent was removed by rotary evaporation. The crude product was transferred to a flask and suspended with ethyl acetate. A solution of potassium carbonate (2 g in 10 mL water) was added slowly

to the until the mixture was shown to be basic by litmus. The mixture was stirred vigorously and propionyl chloride (3 x 0.2 mL) was added waiting 10 minutes between additions. The organic layer was collected, dried over anhydrous sodium sulfate, filtered through cotton, and the solvent evaporated. This crude product was used in the next step without purification.

N-methyl imidazole-amide cavitand 2:

Crude chloro-amide cavitand (75 mg, 0.045 mmol) was placed in a round-bottomed flask with excess N-methyl-imidazole (2 mL) and a stir bar and the reaction was stirred at 90 °C for 16 h. The reaction was cooled and cold acetone (2 mL) was added to form a pale-yellow precipitate which was filtered and collected. The solid was then refluxed in acetone (3 mL) for 16 h. The reaction was again cooled and the solid was filtered and dried resulting in cavitand **2** (55 mg, 51% yield) as a pale yellow solid. ^{1}H NMR (400 MHz, D_2O) δ 7.35 (s, 2H), 7.21 (s, 2H), 7.13 (s, 1H), 7.04 (s, 1H), 6.96 (s, 1H), 6.79 (s, 1H), 6.53 (s, 1H), 6.38 (s, 1H), 4.13 (d, J = 7.9 Hz, 2H), 4.05 (d, J = 7.9 Hz, 2H), 3.99 (d, J = 6.8 Hz, 2H), 3.80 (s, 6H), 2.49 (m, 8H), 2.22 (m, 2H), 1.83 (m, 3H), 1.64 (s, 2H), 1.35 (t, J = 7.4 Hz, 6H), 1.22 (t, J = 7.4 Hz, 6H). ^{13}C NMR (150 MHz, D_2O) δ 217.11, 176.78, 176.08, 153.78, 153.00, 145.56, 142.55, 135.68, 133.25, 128.04, 126.12, 123.61, 121.73, 119.48, 115.99, 108.03, 48.32, 35.59, 34.37, 29.71, 29.46, 26.69, 10.12, 9.37. ESI MS: m/z $C_{104}H_{116}N_{16}O_{16}^{4+}$ calculated: 461.2189, found: 461.4691.

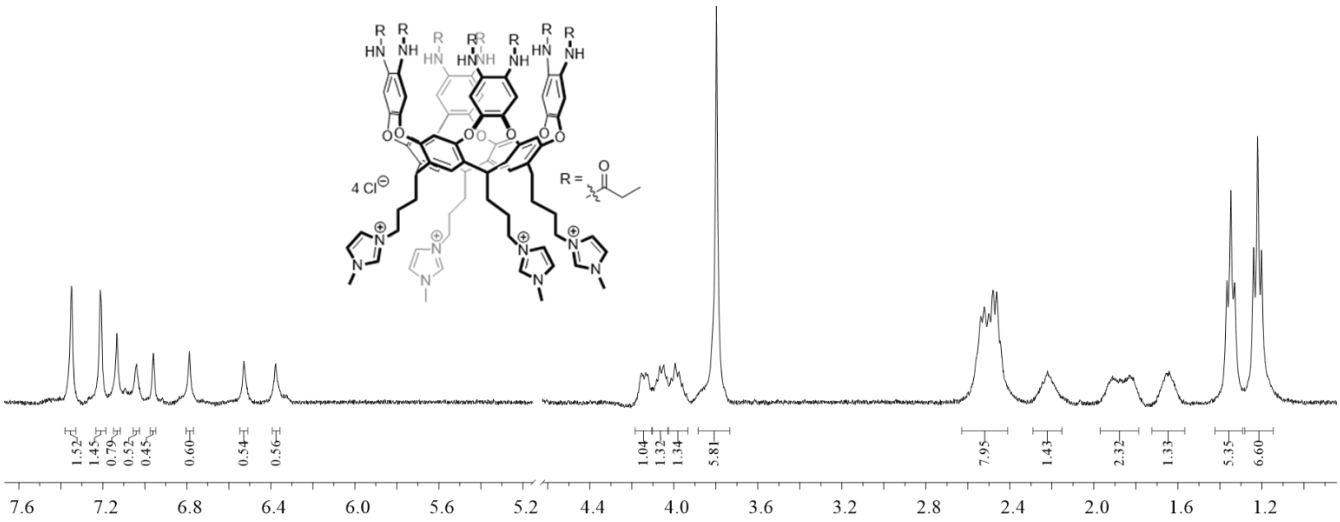

Figure S-1. ^{1}H NMR spectrum of cavitand **2** (400 MHz, D_2O).

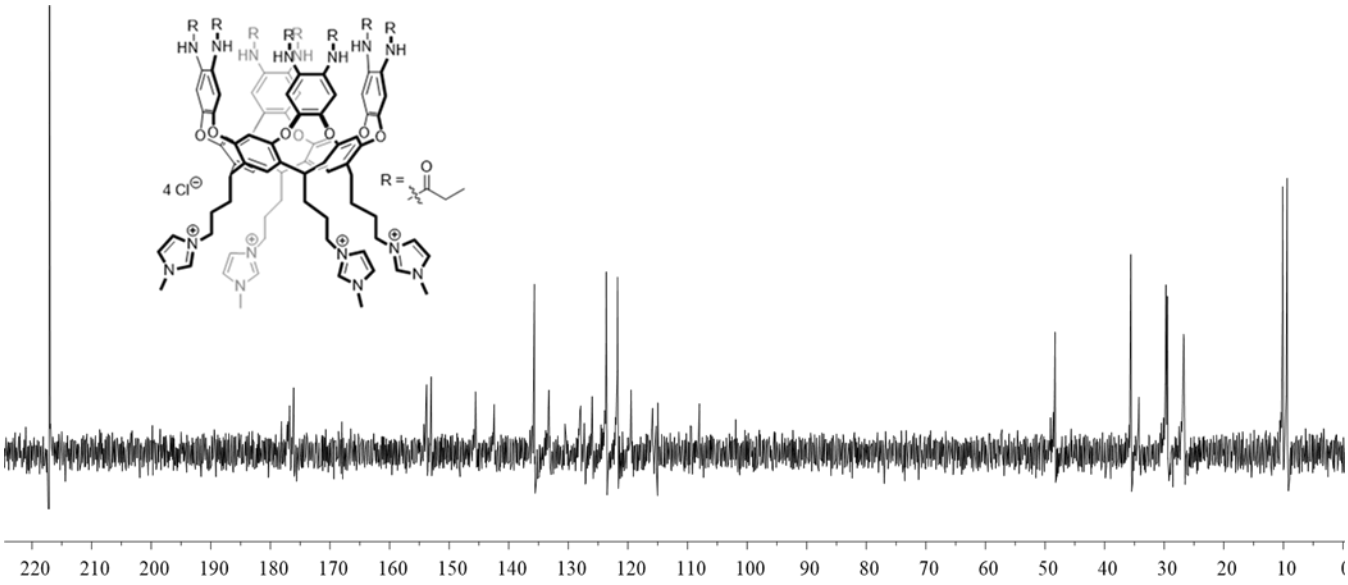

Figure S-2. ^{13}C NMR of cavitand **2** (150 MHz, D_2O).

Styrylpyridinium dye G3:

1,4-Dimethylpyridinium iodide (125 mg, 0.529 mmol) and 4-(1-piperidinyl)benzaldehyde (100 mg, 0.529 mmol) were dissolved in ethanol (3 mL) inside a round bottom flask. While stirring, one drop of piperidine was added and the resulting solution was refluxed for 5 hours. The reaction was cooled, then diluted with water (5 mL). The resulting precipitate was filtered, rinsed with water and cold ethanol, then dried under vacuum to yield (E)-1-methyl-4-(4-(piperidin-1-yl)styryl)pyridin-1-ium iodide **G3** (200 mg, 93% yield) as a dark red powder. ^{1}H NMR (400 MHz, D_2O) δ 8.49 (d, J = 5.6 Hz, 2H), 7.96 (d, J = 5.6 Hz, 2H), 7.76 (d, J = 14.5 Hz, 1H), 7.69 (d, J = 7.3 Hz, 2H), 7.22 (s, 1H), 7.18 (d, J = 7.6 Hz, 2H), 4.24 (s, 3H), 3.28 (m, 4H), 1.71 (m, 4H), 1.63 (d, J = 4.9 Hz, 2H). ^{13}C NMR (150 MHz, D_2O) δ 153.39, 153.46, 143.96, 140.74, 129.60, 123.15, 126.83, 123.15, 119.94, 117.35, 50.35, 46.67, 24.70, 23.43.

ESI MS: m/z $C_{19}H_{23}N_2^+$ calculated 279.1856, found: 279.1862.

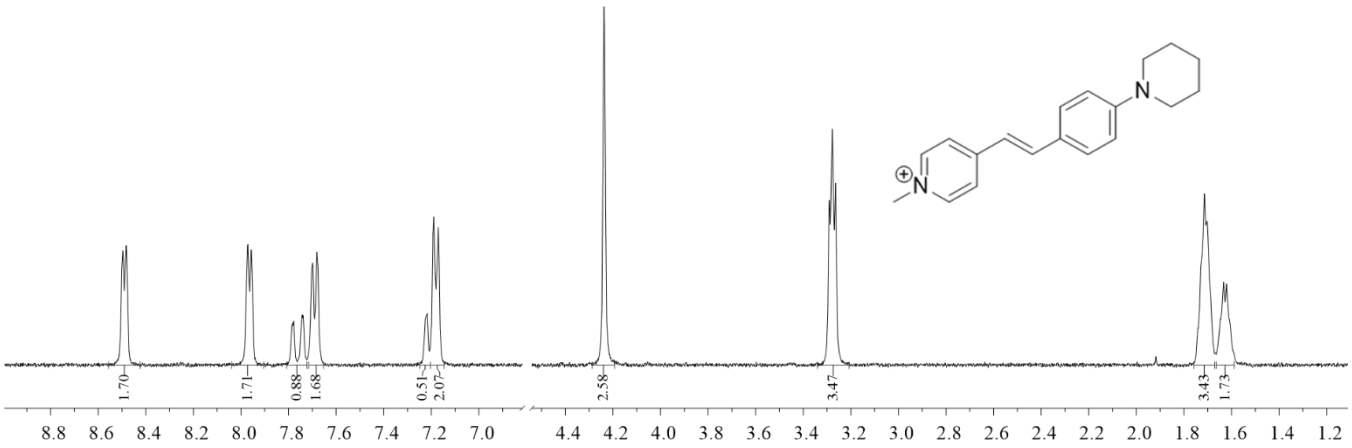

Figure S-3. ^{1}H NMR spectrum of fluorophore **G3** (400 MHz, D_2O).

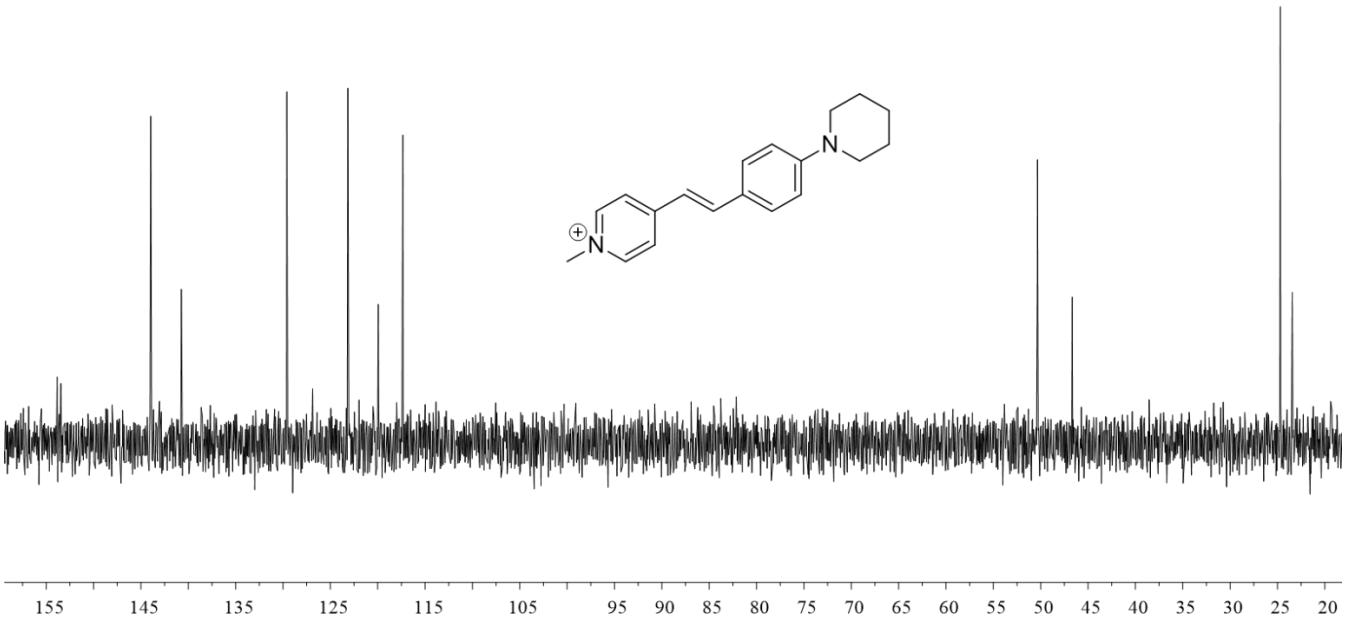

Figure S-4. ^{13}C NMR spectrum of fluorophore **G3** (150 MHz, D_2O).

Peptide Synthesis

Peptides were synthesized on Rink Amide MBHA resin via the standard Fmoc SPPS coupling chemistry either manually or using the CSBio CS336S peptide synthesizer (Menlo Park, CA). All amino acids used were Fmoc protected. Deprotections were run with 20% piperidine in DMF. Coupling of amino acids were performed for at least 60 minutes, with 5 equivalents, and coupling reagents used were DIEA/HBTU in DMF. After coupling, the resin was washed extensively with DMF to remove excess amino acids. Peptides were then cleaved from the beads with deprotected side-chains in a TFA cleavage solution (TFA: TIPS: ddH_2O; 95:2.5:2.5) for 2 h. All peptides were purified on a reverse phase HPLC (DIONEX Ultimate 3000; Thermo Scientific, Idstein, Germany) using a C18 reversed phase preparative column (Kinetex® 5 μm EVO, 250 × 21.2 mm) or a C18 reversed-phase semi-preparative column (Kinetex® 5 μm EVO, 250 × 10 mm), checked for correct mass and impurities using MALDI-TOF MS (AB SCIEX TOF/TOF 5800; Framingham, MA) and analytical HPLC (Kinetex® 2.6 μm EVO, 250 × 4.6 mm), and lyophilized to a powder for long-term storage at -20 ºC.

H3: N'-ARTKQTARKST-C'

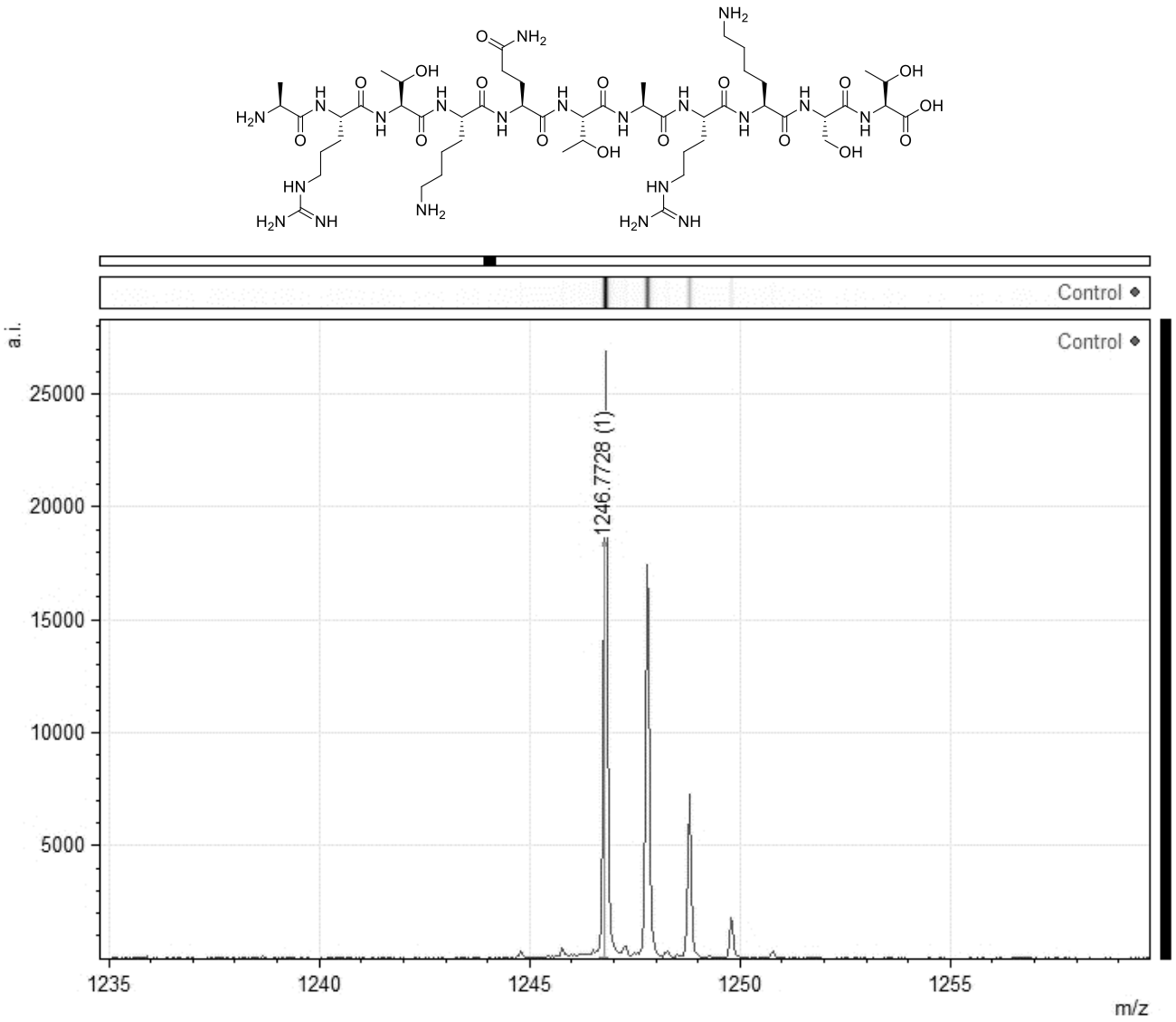

Figure S-5. MALDI-TOF mass spectrum of the H3 (1-11) oligopeptide: m/z $C_{50}H_{94}N_{20}O_{17}^{+}$ calculated 1246.7106, found: 1246.7728.

H3R2$_{Ci}$: **N'-AR$_{Ci}$TKQTARKST-C'**

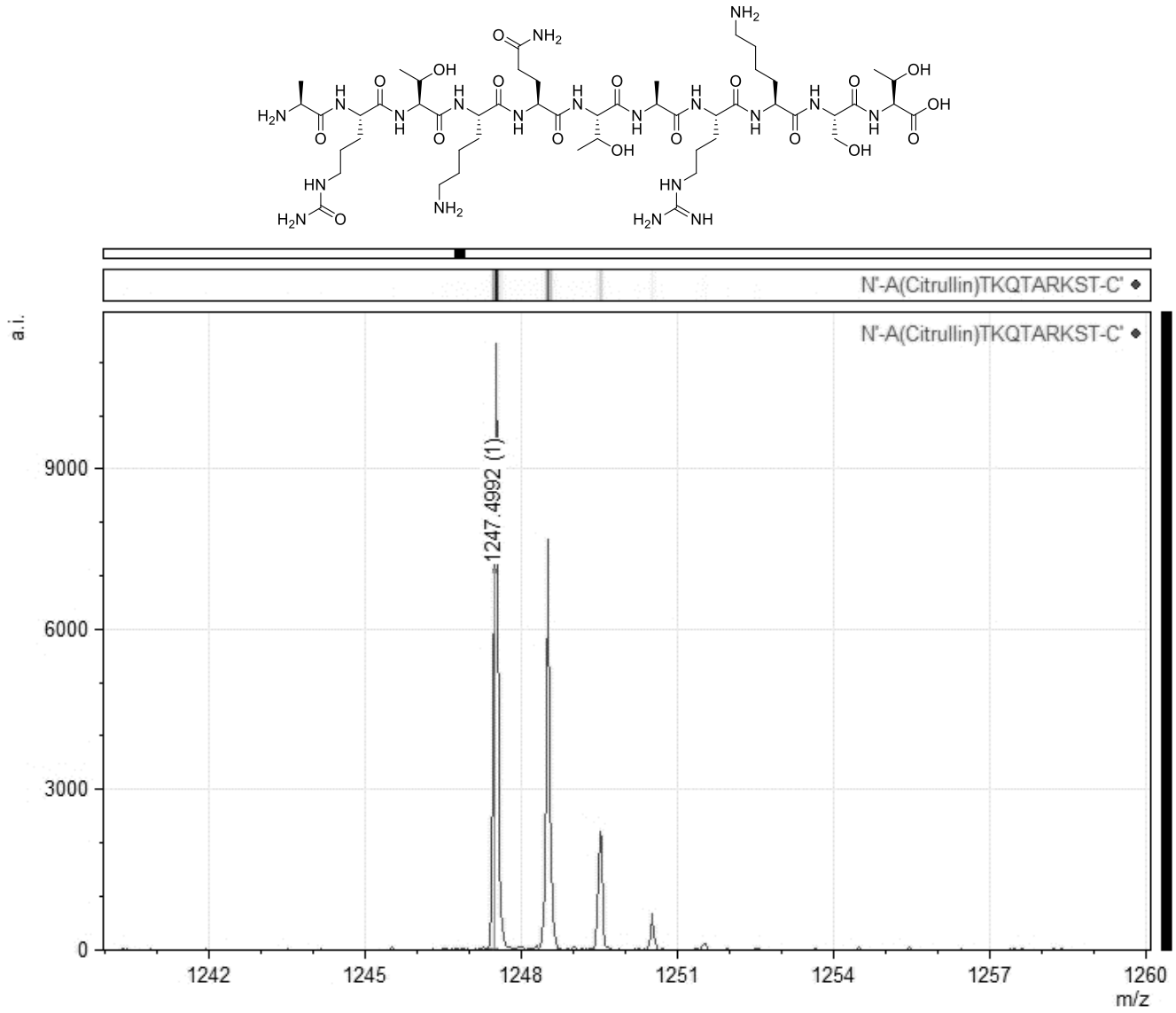

Figure S-6. MALDI-TOF mass spectrum of the H3R2$_{Ci}$ (1-11) oligopeptide: m/z $C_{50}H_{93}N_{19}O_{18}^{+}$ calculated 1247.6946, found: 1247.4992.

H3R8$_{Ci}$: N'-ARTKQTAR$_{Ci}$KST-C'

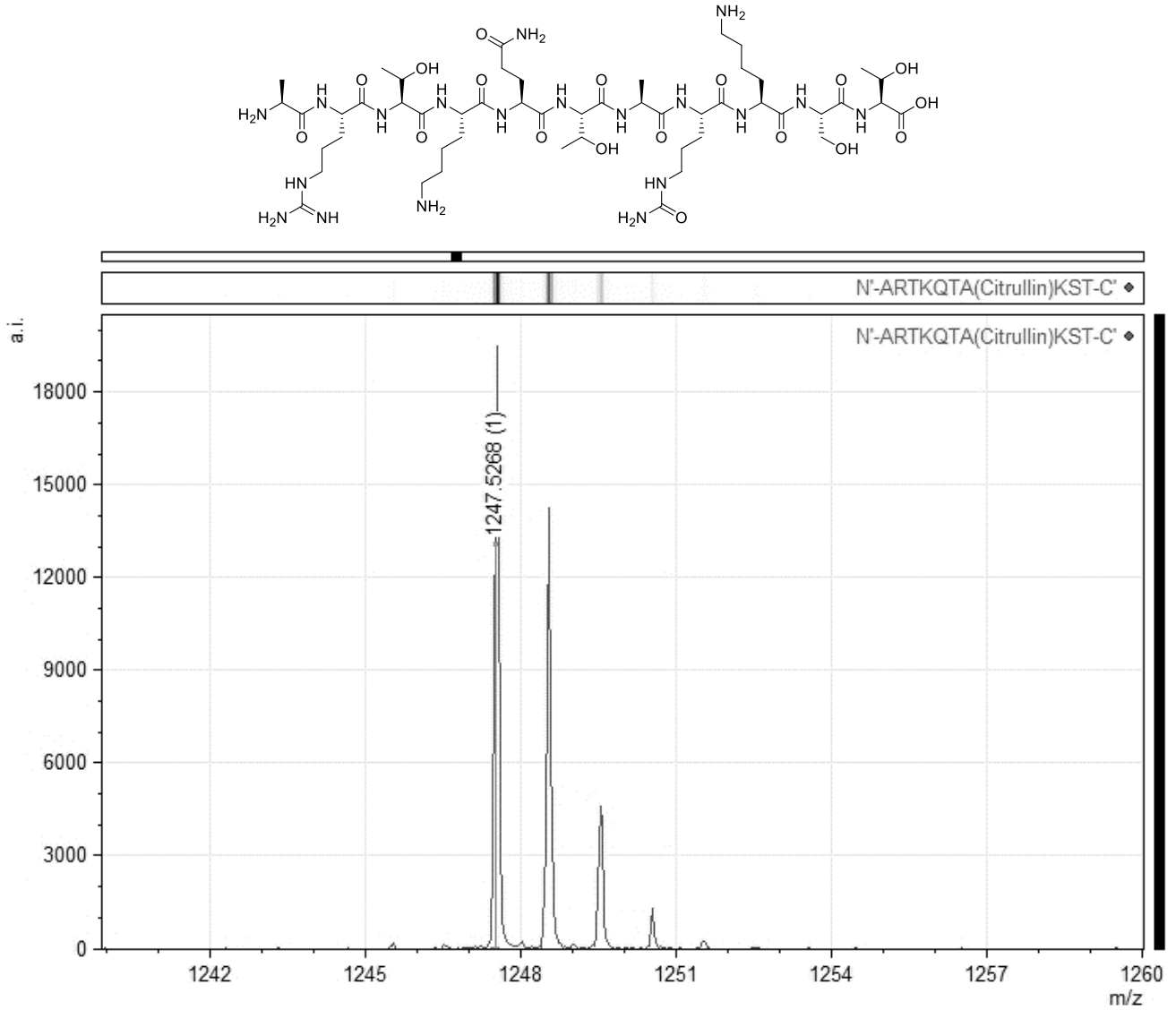

Figure S-7. MALDI-TOF mass spectrum of the H3R8$_{Ci}$ (1-11) oligopeptide: m/z $C_{50}H_{93}N_{19}O_{18}^{+}$ calculated 1247.6946, found: 1247.5268.

H3R2$_{Ci}$R8$_{Ci}$: N'-AR$_{Ci}$TKQTAR$_{Ci}$KST-C'

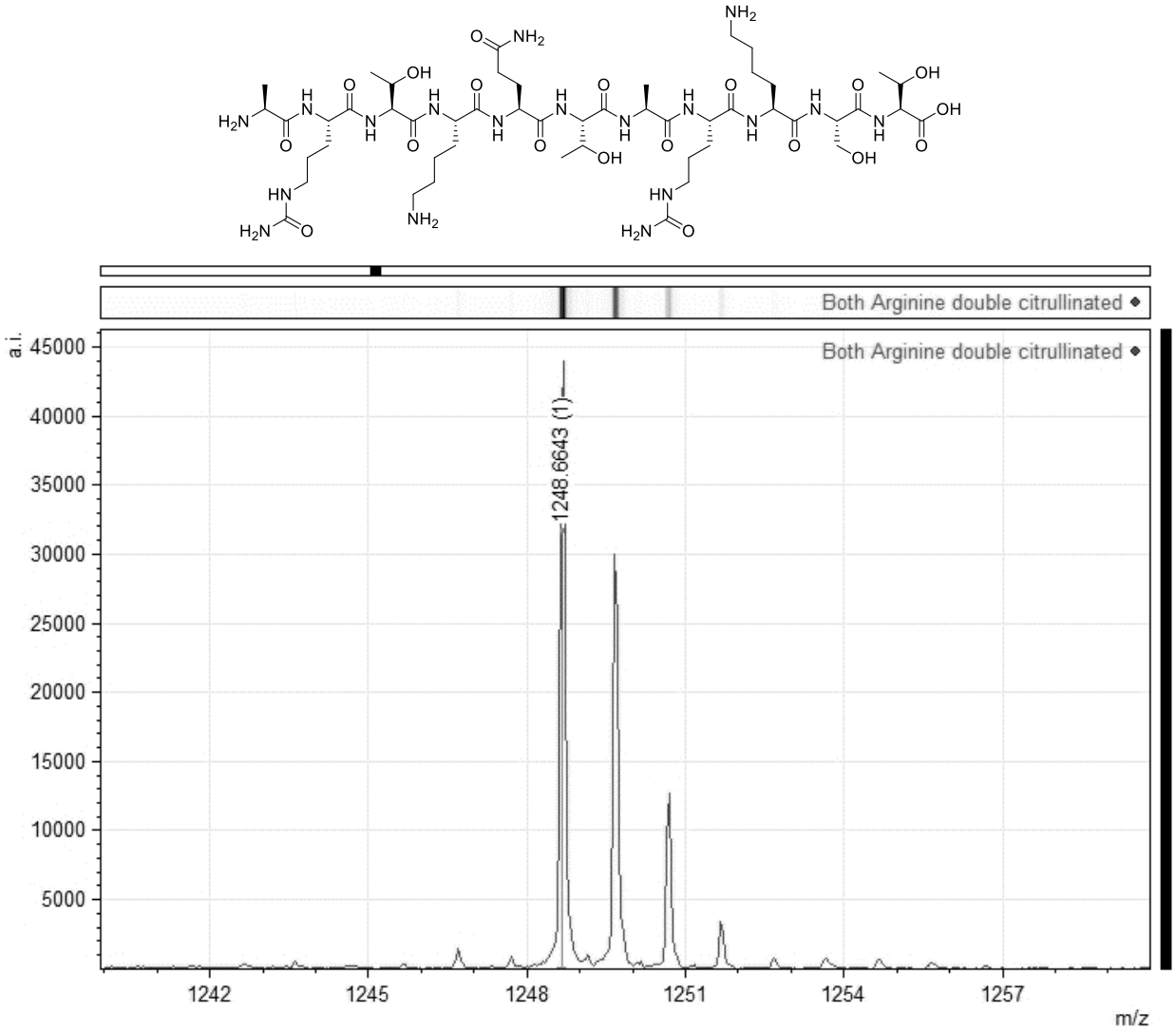

Figure S-8. MALDI-TOF mass spectrum of the H3R2$_{Ci}$R8$_{Ci}$ (1-11) oligopeptide: m/z $C_{50}H_{92}N_{18}O_{19}^{+}$ calculated 1248.6786, found: 1248.6643.

3. Experimental Procedures

Fluorescence measurements.

In general, the fluorescence assays were carried out by mixing 10 µL of the fluorescent guest **G1, G2,** or **G3** (30 µM, 15 µM, or 15 µM), 10 µL of cavitand **1** or **2** (200 µM), 10 µL metal salts (100 µM in water), 60 µL of the incubation buffer (Tris buffer HCl, pH 7.4, 20 mM, Bis Tris buffer, pH 5.5, 20 mM, or Citrate buffer, pH 3.3, 20 mM) in the 96-well plate, adding 10 µL of the peptide solution at 100 µM to bring the total volume up to 100 µL, and incubating with mild shaking for 15 mins at room temperature. Each experimental condition was repeated in quadruplicate, using identical sensor components across four wells, and collecting fluorescence signals for each. The fluorescence signal (F) was recorded in a Bio-Tek Synergy HT Multi-Detection Microplate Reader, or a Perkin Elmer Wallac 1420 Victor 2 Microplate Reader (PerkinElmer), with the Ex/Em wavelengths at 530/605 nm for guest **G1** and 485/605 nm for guests **G2** and **G3**.

Data analysis. The quadruplicate raw fluorescence data sets were subjected to Linear Discriminant Analysis (LDA) and Principal Component Analysis (PCA) performed with RStudio (Version 1.0.136), an integrated development environment (IDE) for R (version 3.3.2). Scores plots and confidence intervals were graphed in RStudio using the packages ggplot2, ggpubr, and ggfortify. All other fluorescence data charts were created in Microsoft Excel, with values representing the mean of the quadruplicate responses and error bars indicating their standard deviation.

4. Spectroscopic Analysis

NMR Analysis of Host:Guest Binding

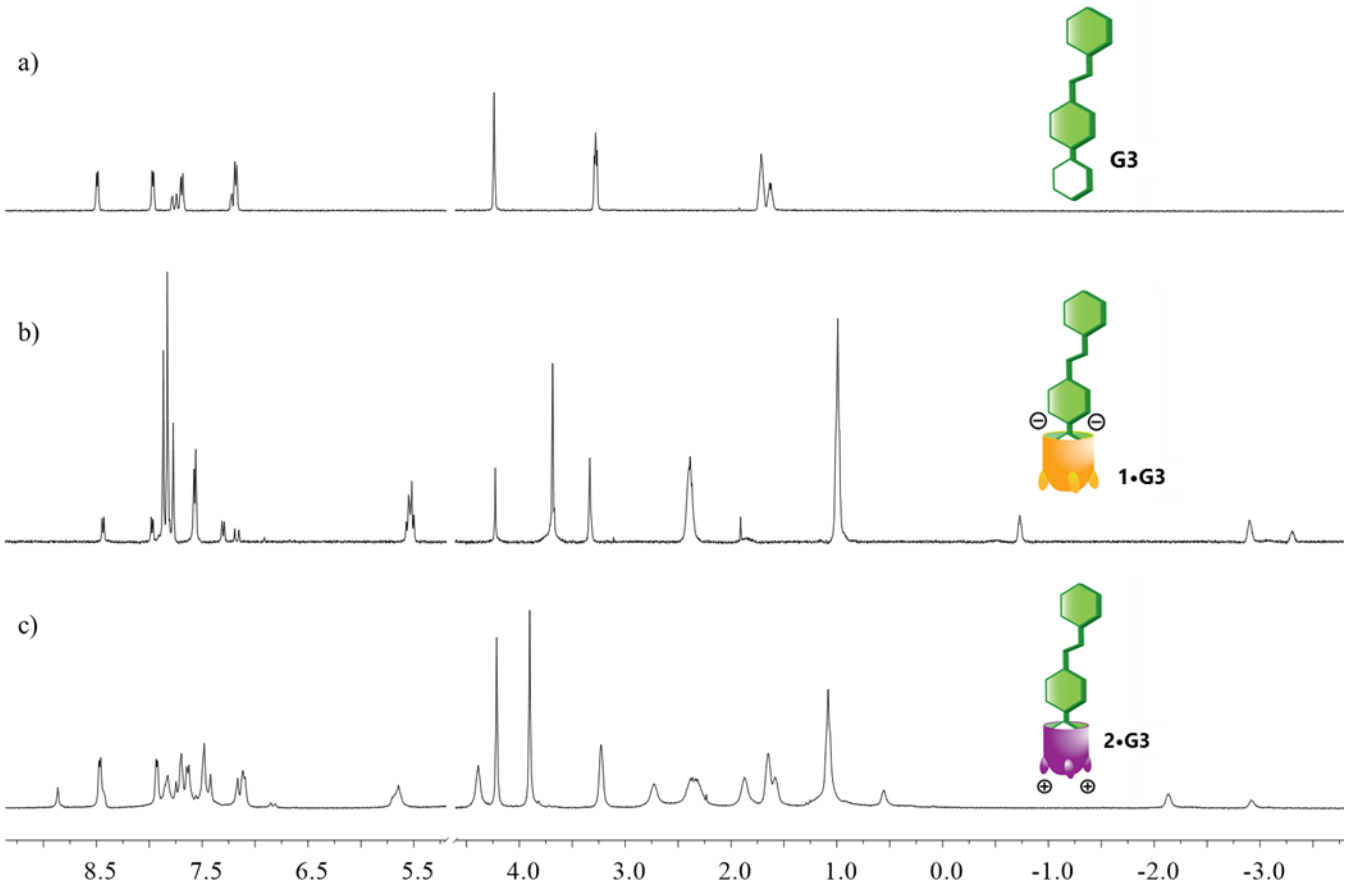

Figure S-9. ^{1}H NMR spectra (400 MHz, D_2O) of a) guest **G3**; b) guest **G3** binding in host **1**; c) guest **G3** binding in host **2**.

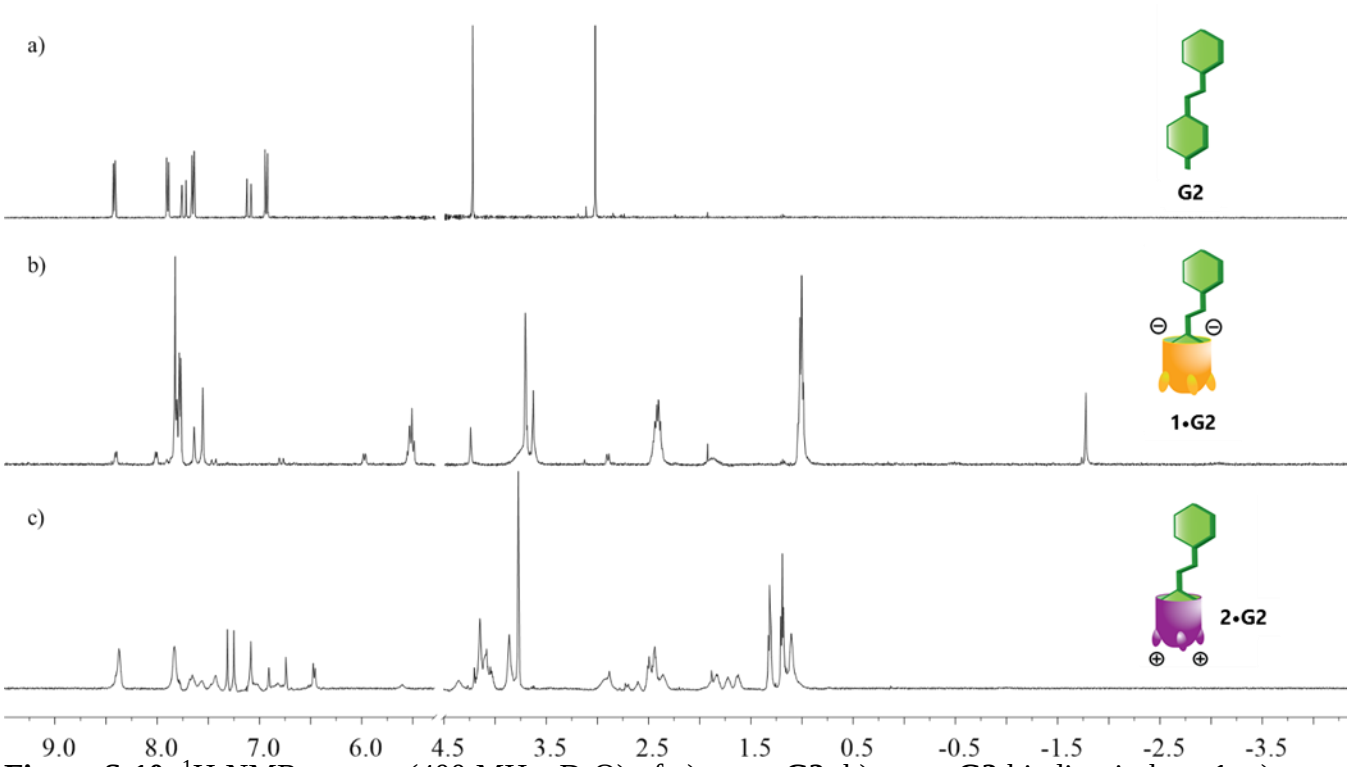

Figure S-10. ^{1}H NMR spectra (400 MHz, D_2O) of a) guest **G2**; b) guest **G2** binding in host **1**; c) guest **G2** in rapid exchange with host **2**.

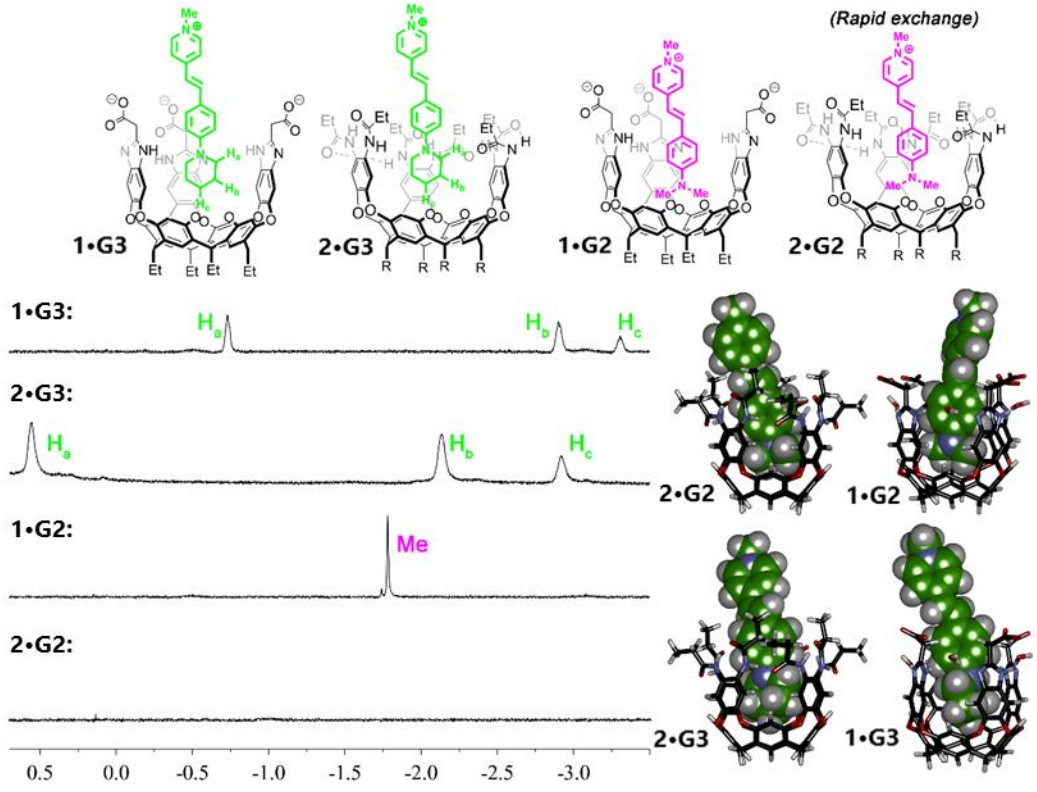

Figure S-11. Upfield regions of the ^{1}H NMR spectra of host:guest complexes **1•G2**, **2•G2**, **1•G3**, **2•G3**, (400 MHz, D_2O), showing the position of the guest in the cavity, and minimized structures (SPARTAN, Hartree-Fock) of the complexes.

Optimization of Indicator Assay

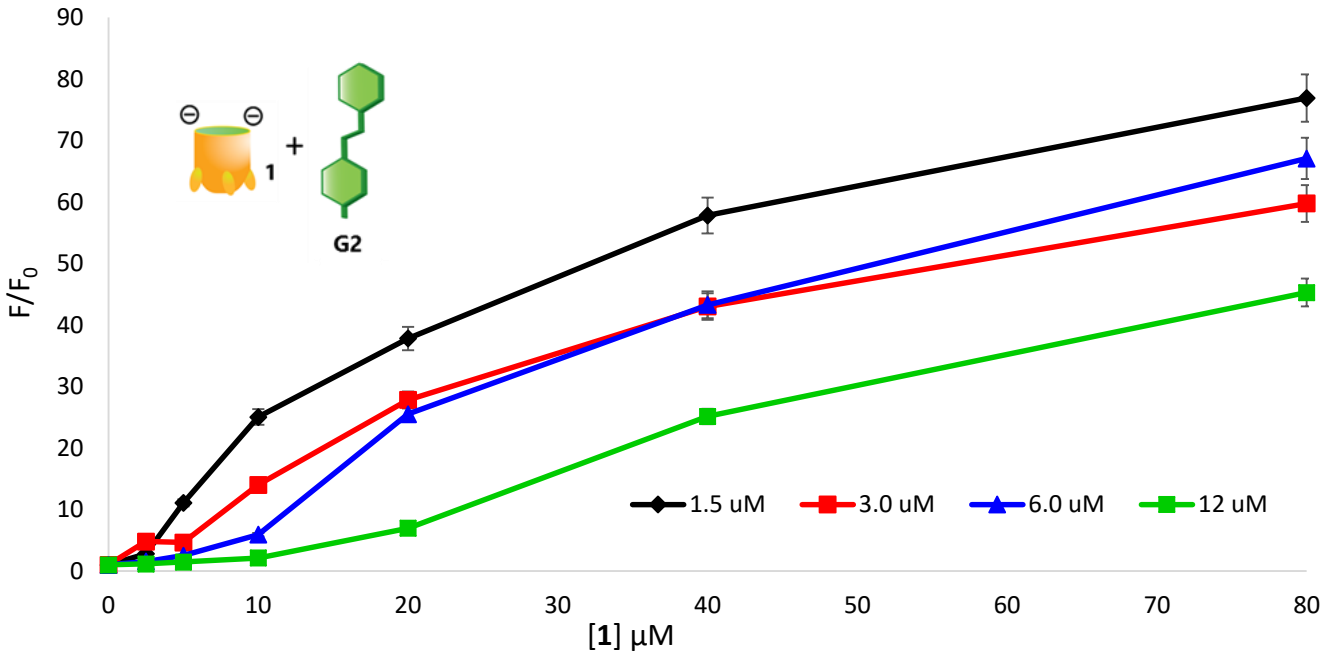

Figure S-12. Concentration Dependence. Fluorescence response curves of the **1•G2** complex in 20 mM Tris buffer, pH 7.4. The concentration of host **1** was increased in the presence of various [**G2**]. F_0 = fluorescence response of **G2**, F = fluorescence response of **1•G2**.

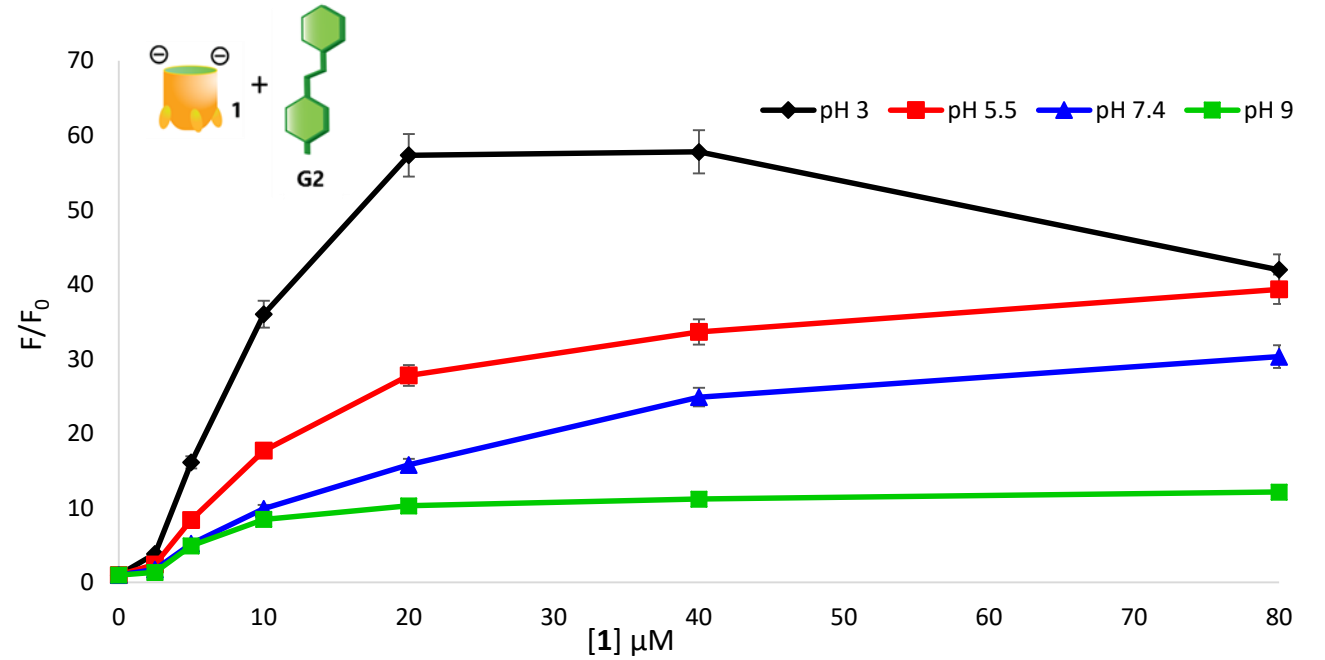

Figure S-13. pH Dependence. Fluorescence response curves of the **1•G2** complex in 20 mM citrate, BisTris, Tris, or carbonate buffer, at pH 3.3, 5.5, 7.4, or 9.0, respectively. [**1**] was increased in the presence of 1.5 µM fluorophore **G2**. F_0 = fluorescence response of **G2**, F = fluorescence response of **1•G2**.

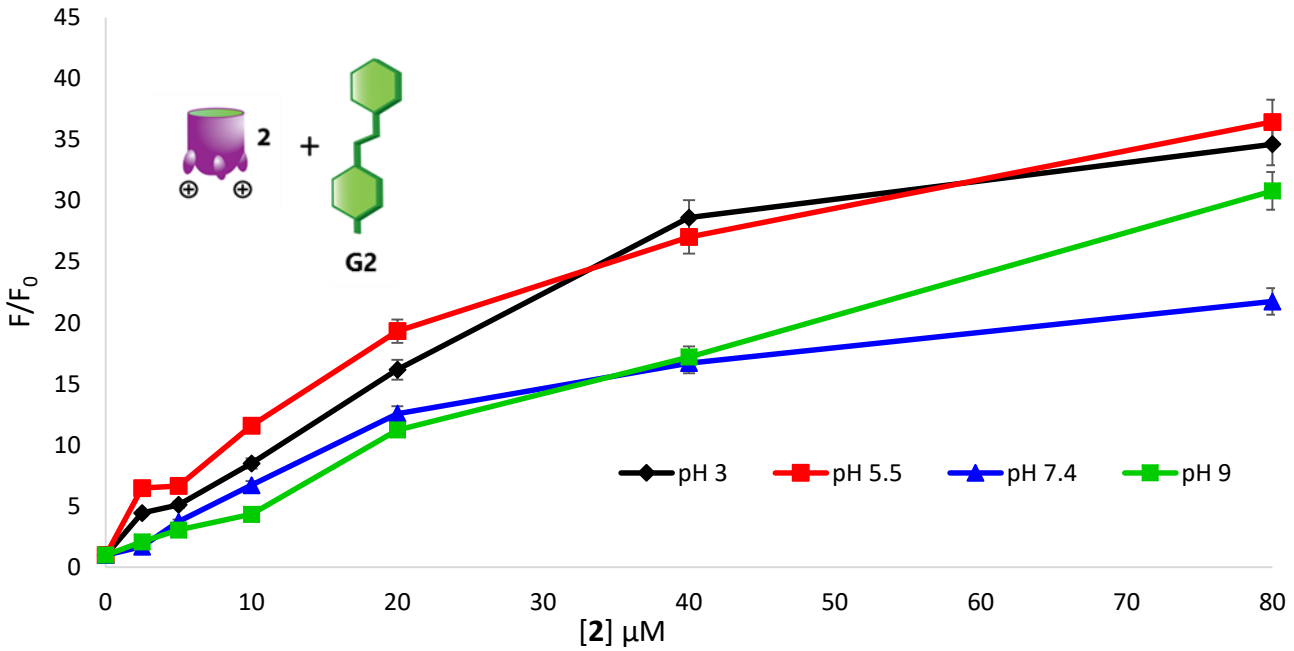

Figure S-14. pH Dependence. Fluorescence response curves of the **2•G2** complex in 20 mM citrate, BisTris, Tris, or carbonate buffer, at pH 3.3, 5.5, 7.4, or 9.0, respectively. [**2**] was increased in the presence of 1.5 µM fluorophore **G2**. F_0 = fluorescence response of **G2**, F = fluorescence response of **2•G2**.

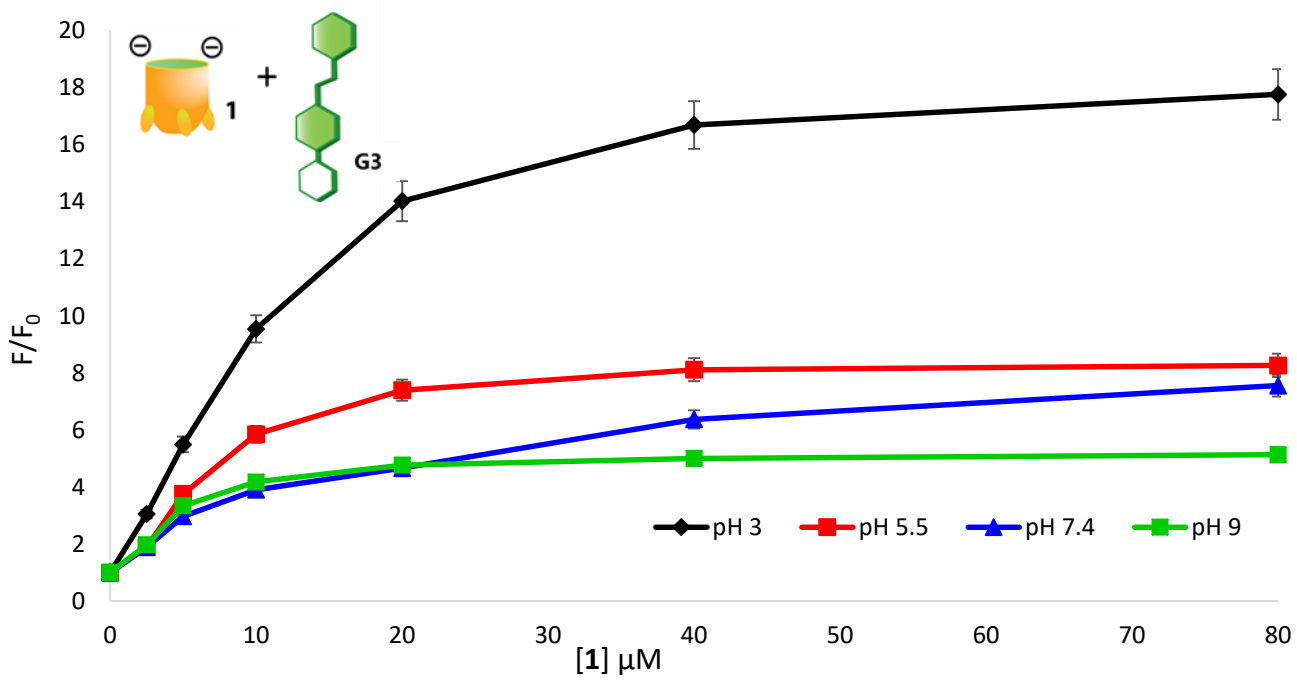

Figure S-15. pH Dependence. Fluorescence response curves of the **1•G3** complex in 20 mM citrate, BisTris, Tris, or carbonate buffer, at pH 3.3, 5.5, 7.4, or 9.0, respectively. [**1**] was increased in the presence of 1.5 µM fluorophore **G3**. F_0 = fluorescence response of **G3**, F = fluorescence response of **1•G3**.

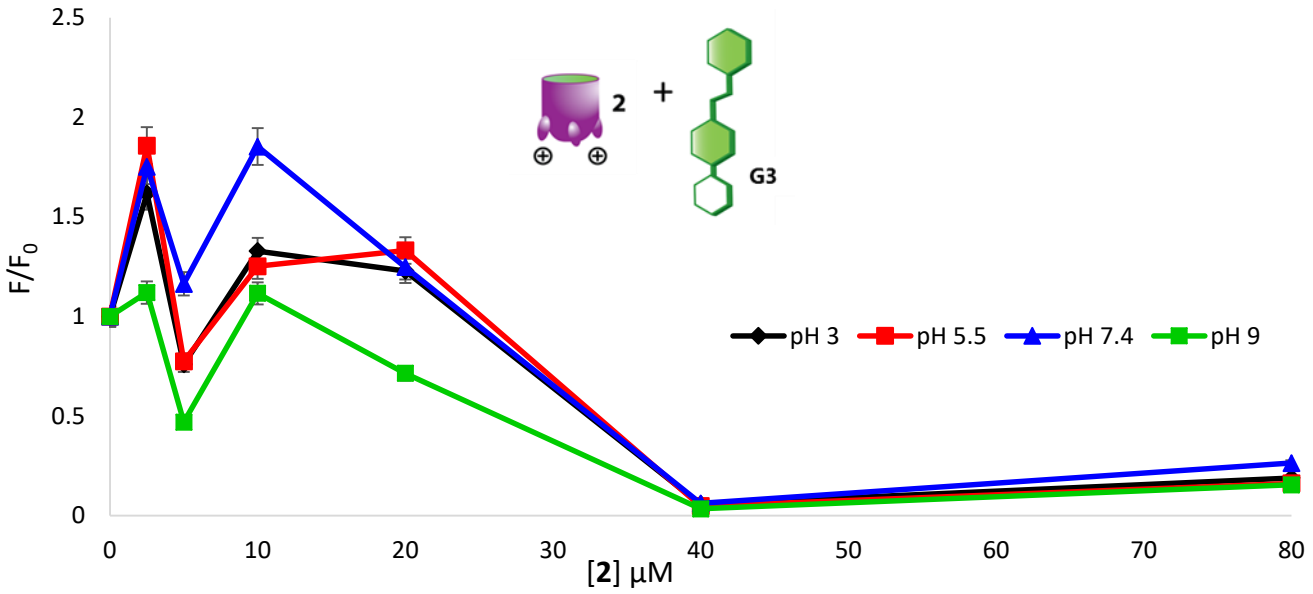

Figure S-16. pH Dependence. Fluorescence response curves of the **2•G3** complex in 20 mM citrate, BisTris, Tris, or carbonate buffer, at pH 3.3, 5.5, 7.4, or 9.0, respectively. [**2**] was increased in the presence of 1.5 µM fluorophore **G3**. F_0 = fluorescence response of **2**, F = fluorescence response of **2•G3**.

Sensor Calibrations

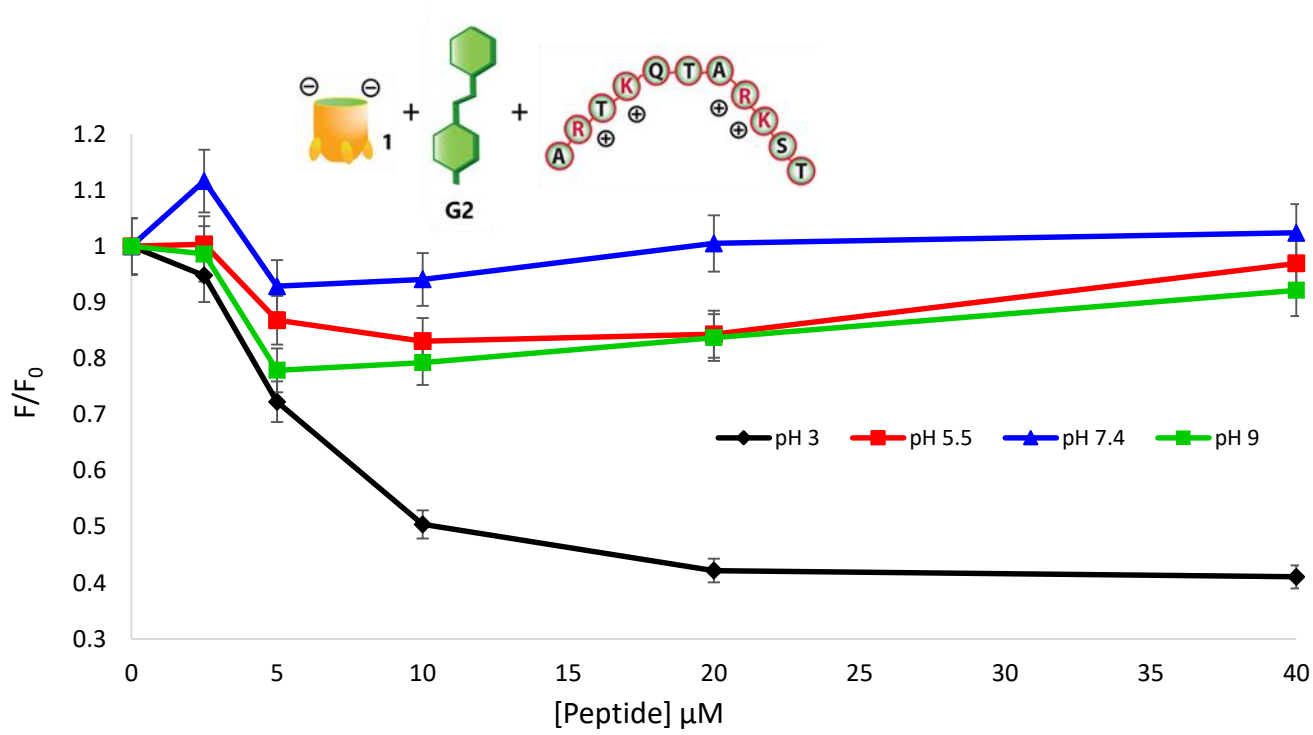

Figure S-17. Fluorescence response of the **1•G2** complex to unmodified H3 peptides in 20 mM citrate, BisTris, Tris, or carbonate buffer, at pH 3.3, 5.5, 7.4, or 9.0, respectively. [peptide] was increased in the presence of 1.5 µM fluorophore **G2** and 20 µM guest **1**. F_0 = fluorescence response of the **1•G2** complex, F = fluorescence response in the presence of H3 peptide.

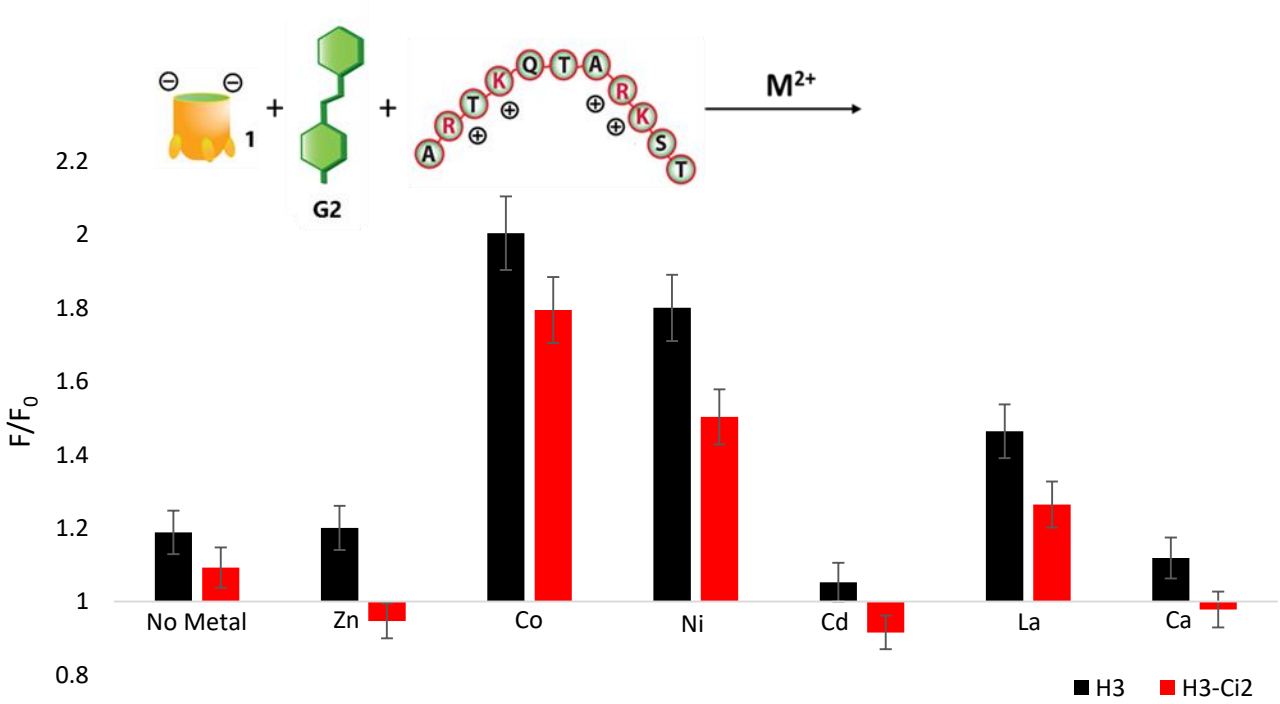

Figure S-18. Effect of metal addition to the **1•G2•**peptide complex in 20 mM Tris buffer, pH 7.4. [**1**] = 20 μM, [**G2**] = 1.5 μM, [Metal] = 10 μM, [Peptides] = 10 μM.

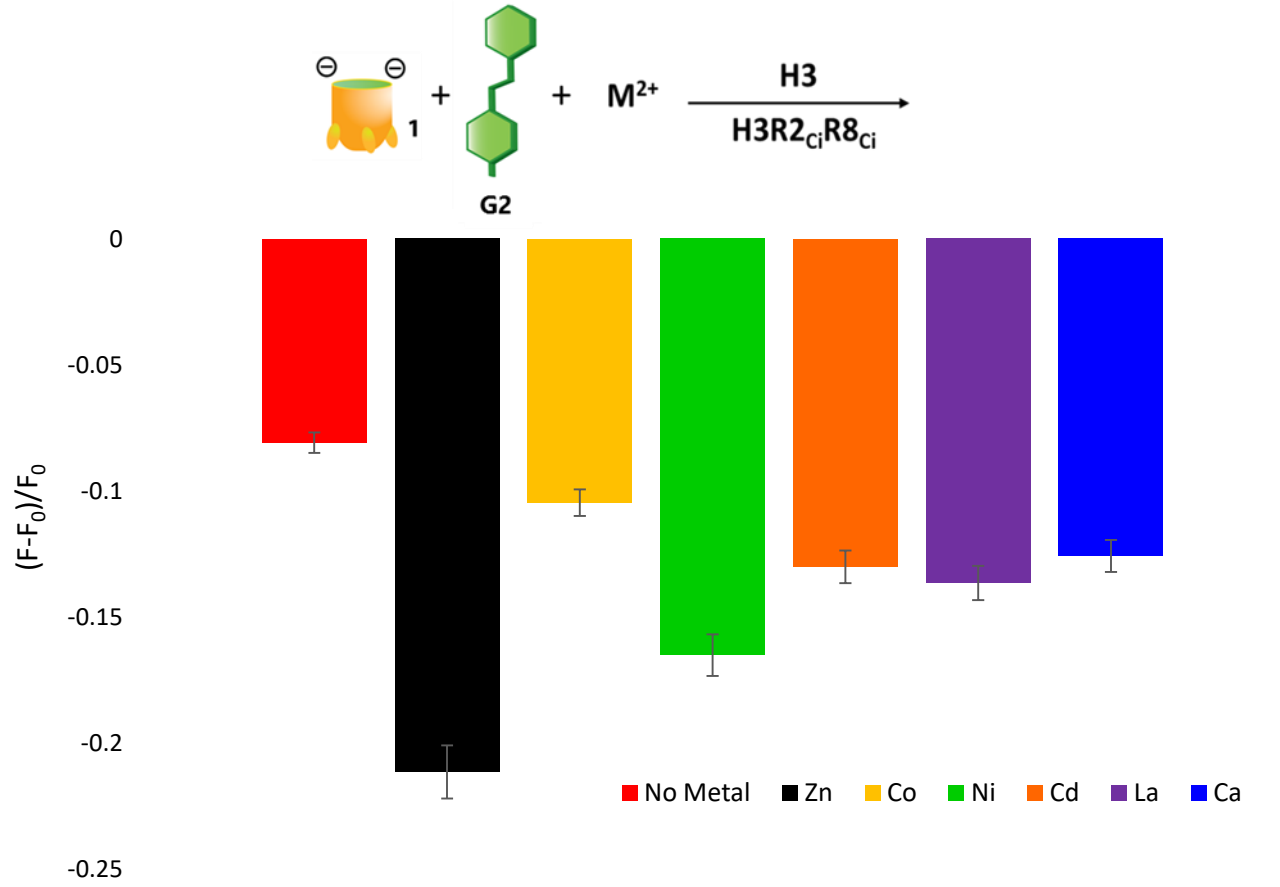

Figure S-19. Relative fluorescence responses of the **1•G2•M^{2+}•**peptide complex in 20 mM Tris buffer, pH 7.4. [**1**] = 20 μM, [**G2**] = 1.5 μM, [Metal] = 10 μM, [Peptides] = 10 μM. F_0 = fluorescence response of the **1•G2•H3** complex, F = fluorescence response of the **1•G2•H3R2$_{Ci}$R8$_{Ci}$** complex.

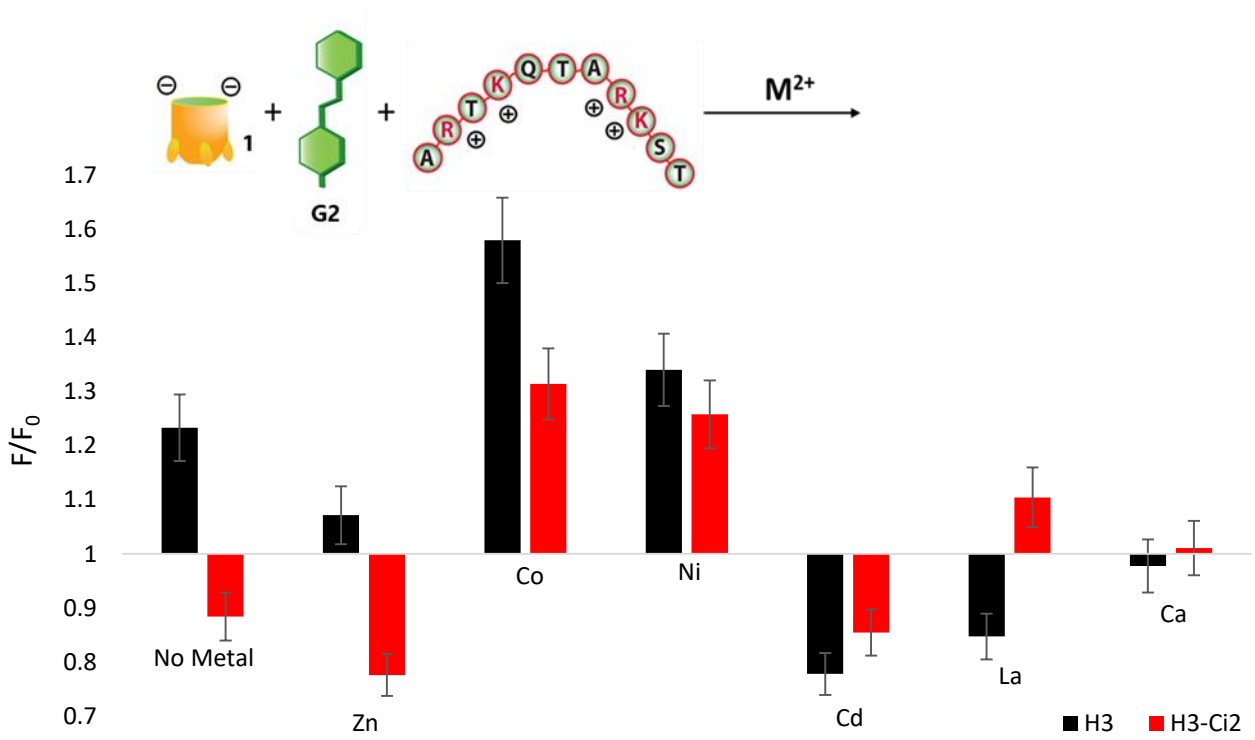

Figure S-20. Effect of metal addition to the **1•G2•**peptide complex in 20 mM BisTris buffer, pH 5.5. [**1**] = 20 μM, [**G2**] = 1.5 μM, [Metal] = 10 μM, [Peptides] = 10 μM.

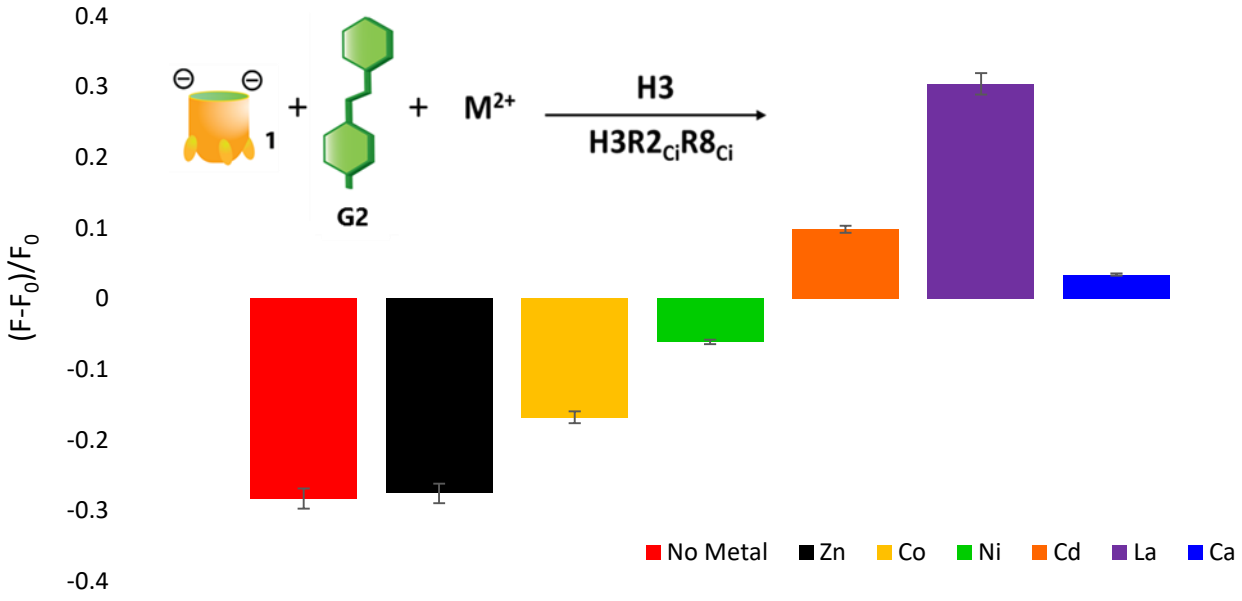

Figure S-21. Relative fluorescence responses of the **1•G2•M^{2+}•**peptide complex in 20 mM BisTris buffer, pH 5.5. [**1**] = 20 μM, [**G2**] = 1.5 μM, [Metal] = 10 μM, [Peptides] = 10 μM. F_0 = fluorescence response of the **1•G2•H3** complex, F = fluorescence response of the **1•G2•H3R2$_{Ci}$R8$_{Ci}$** complex.

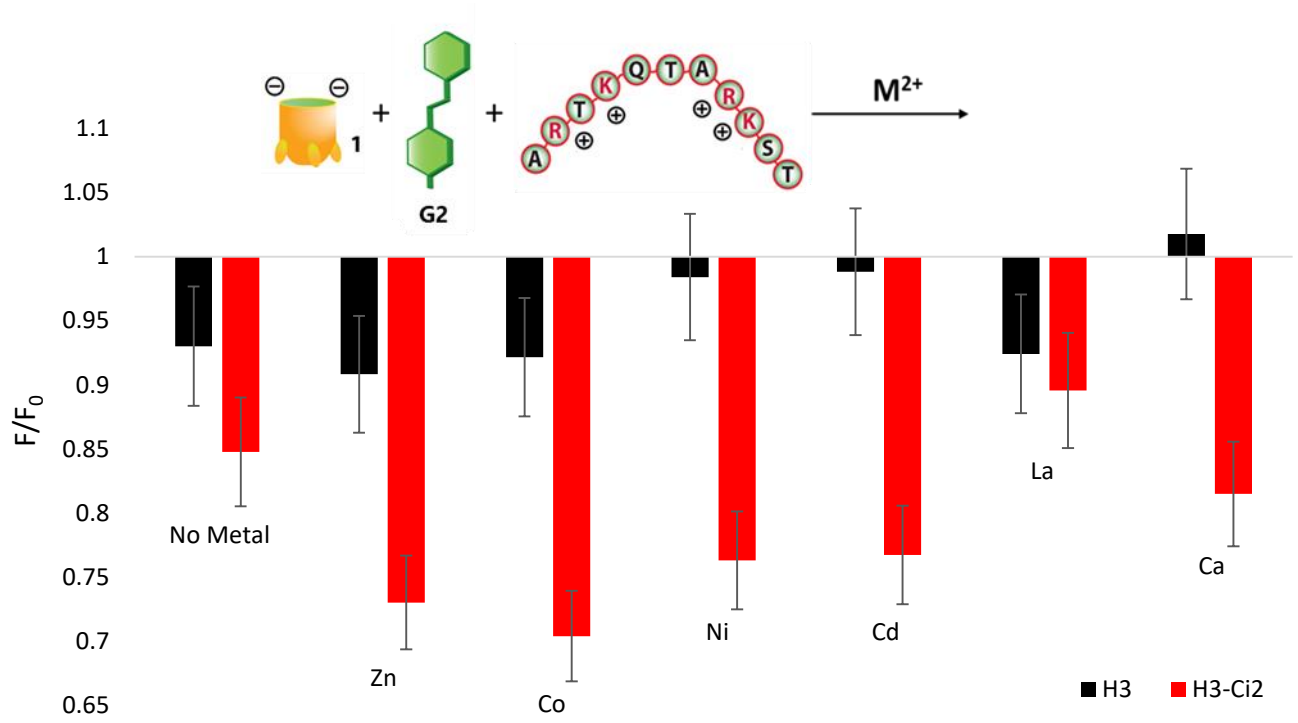

Figure S-22. Effect of metal addition to the **1•G2•**peptide complex in 20 mM citrate buffer, pH 3.3. [**1**] = 20 μM, [**G2**] = 1.5 μM, [Metal] = 10 μM, [Peptides] = 10 μM.

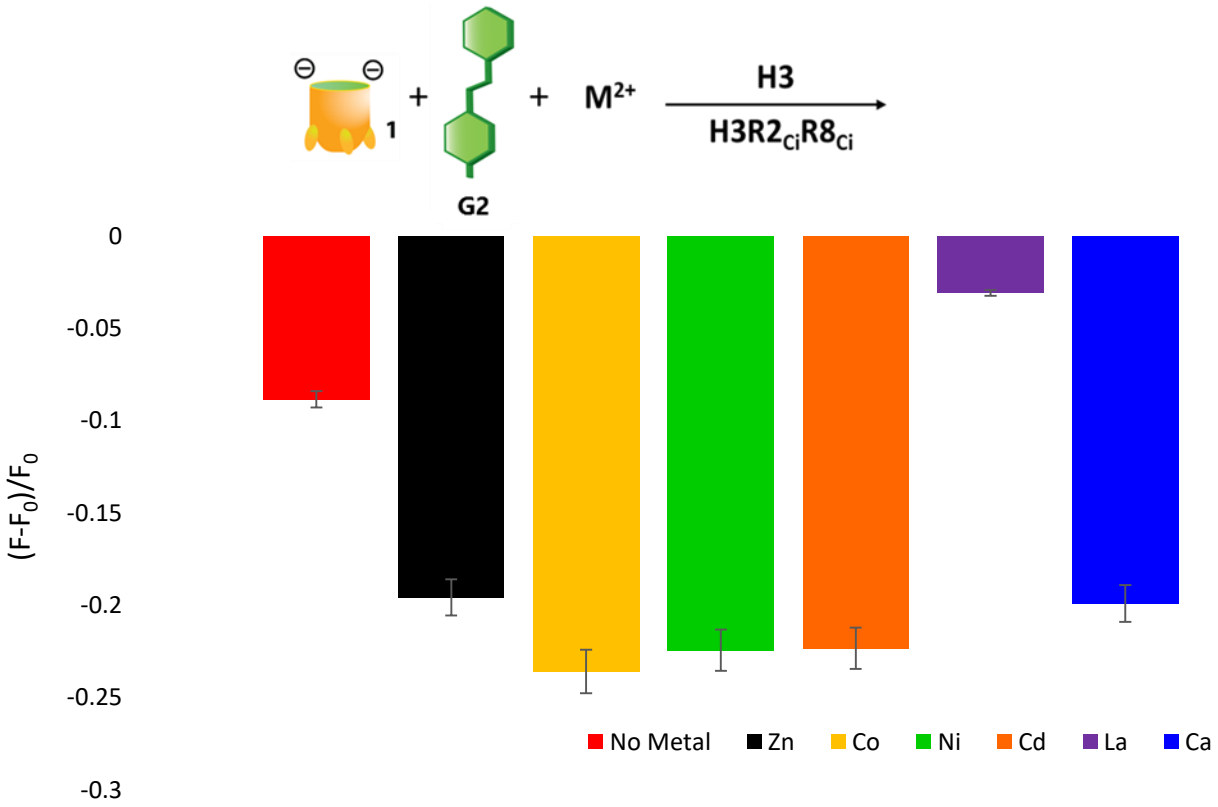

Figure S-23. Relative fluorescence responses of the **1•G2•M^{2+}•**peptide complex in 20 mM citrate buffer, pH 3.3. [**1**] = 20 μM, [**G2**] = 1.5 μM, [Metal] = 10 μM, [Peptides] = 10 μM. F_0 = fluorescence response of the **1•G2 •M^{2+}•H3** complex, F = fluorescence response of the **1•G2•M^{2+}•H3R2$_{Ci}$R8$_{Ci}$** complex.

1•G1 Sensor Responses to H3 Peptides

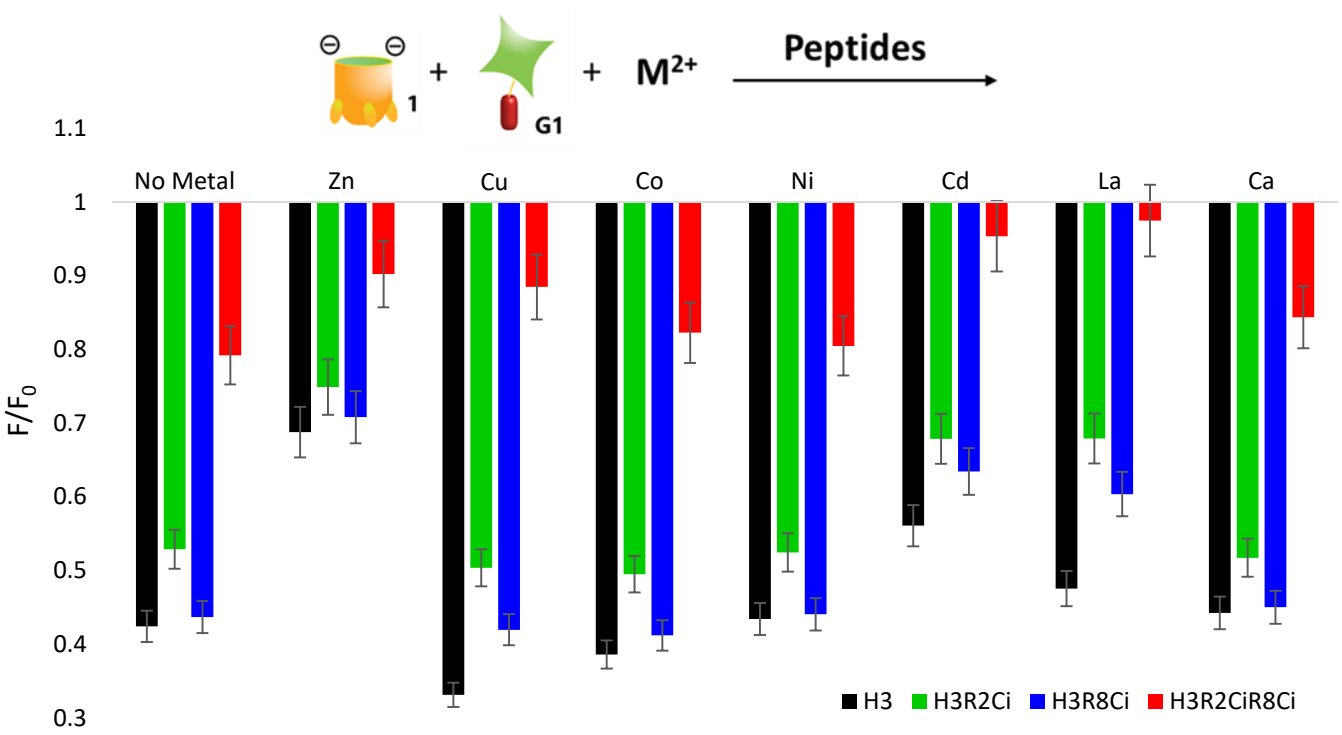

Figure S-24. Relative fluorescence responses of the **1•G1•M^{2+}** complex in 20 mM Tris buffer, pH 7.4. [**1**] = 20 μM, [**G1**] = 3.0 μM, [Metal] = 10 μM, [Peptides] = 10 μM. F_0 = fluorescence response of the **1•G1•M^{2+}** complex, F = fluorescence response of the **1•G1•M^{2+}•Peptide** complex.

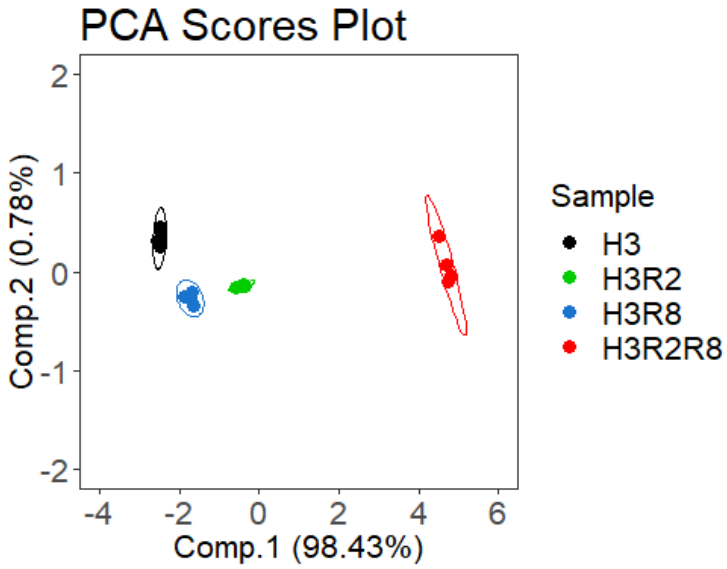

Figure S-25. PCA scores plot with 95% confidence intervals for the 8-factor **1•G1•M^{2+}•Peptide** sensor array (obtained from PCA of data in Figure S-24). [**1**] = 20 μM, [**G1**] = 3.0 μM, [Metal] = 10 μM, [Peptides] = 10 μM, [Tris] = 20 mM (pH 7.4).

1•G2 Sensor Responses to H3 Peptides

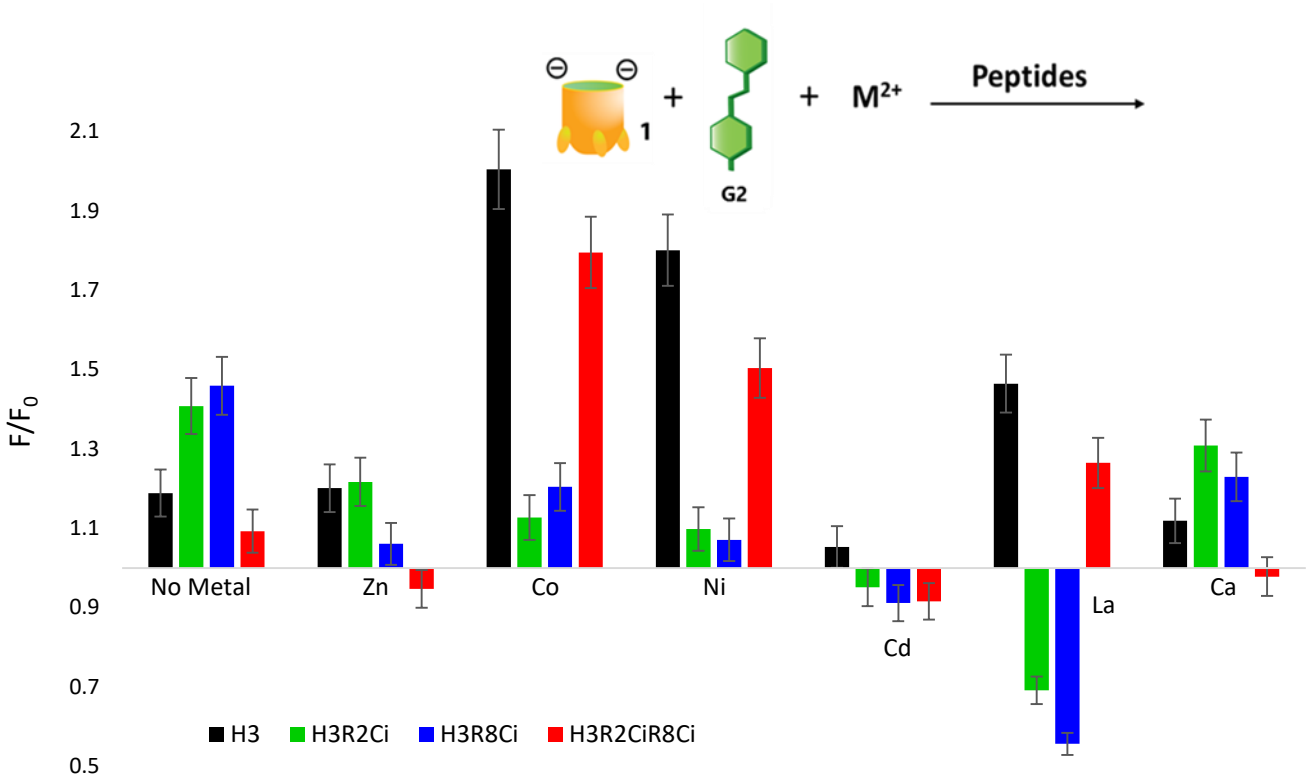

Figure S-26. Relative fluorescence responses of the **1•G2•M**$^{2+}$ complex in 20 mM Tris buffer, pH 7.4. [**1**] = 20 μM, [**G2**] = 1.5 μM, [Metal] = 10 μM, [Peptides] = 10 μM. F_0 = fluorescence response of the **1•G2•M**$^{2+}$ complex, F = fluorescence response of the **1•G2•M**$^{2+}$**•Peptide** complex.

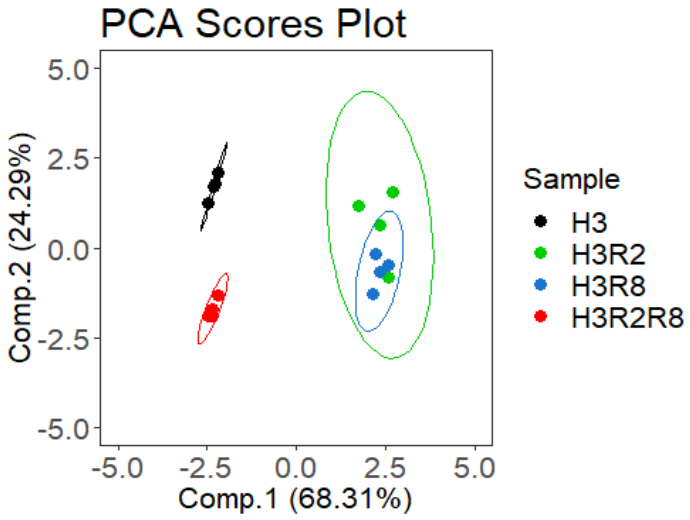

Figure S-27. PCA scores plot with 95% confidence intervals for the 7-factor **1•G2•M**$^{2+}$**•Peptide** sensor array (obtained from PCA of data in Figure S-26). [**1**] = 20 μM, [**G2**] = 1.5 μM, [Metal] = 10 μM, [Peptides] = 10 μM, [Tris] = 20 mM (pH 7.4).

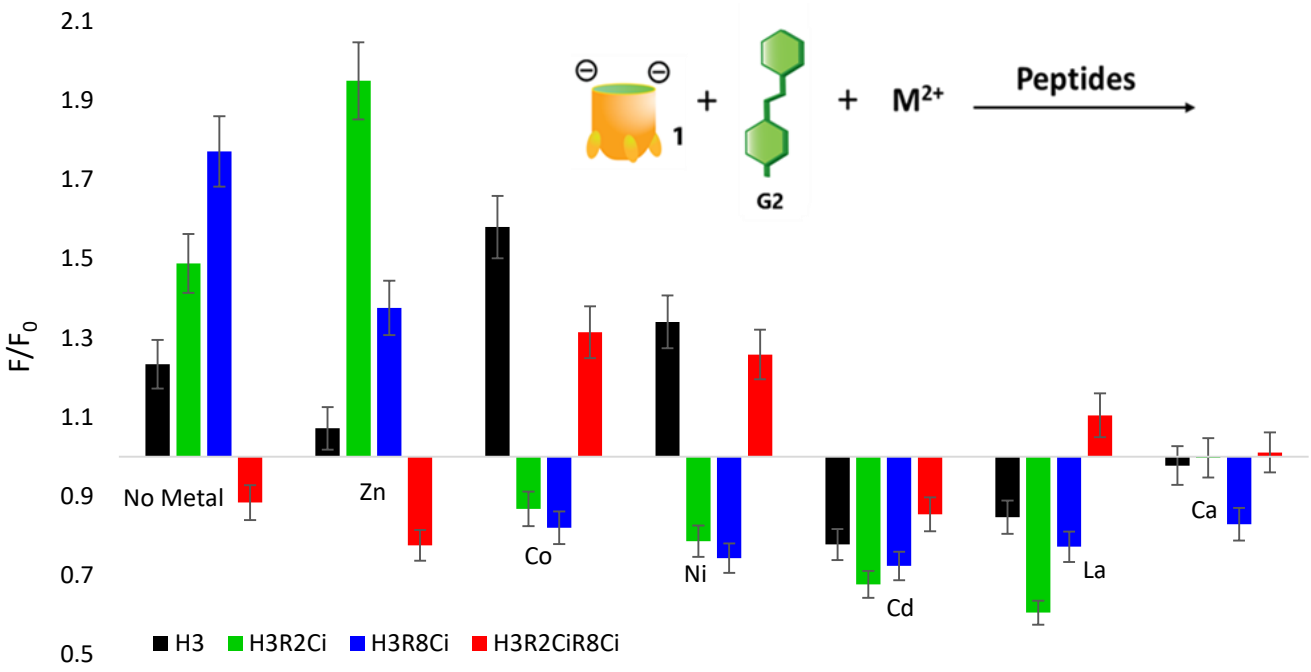

Figure S-28. Relative fluorescence responses of the **1•G2•M**$^{2+}$ complex in 20 mM BisTris buffer, pH 5.5. [**1**] = 20 μM, [**G2**] = 1.5 μM, [Metal] = 10 μM, [Peptides] = 10 μM. F_0 = fluorescence response of the **1•G2•M**$^{2+}$ complex, F = fluorescence response of the **1•G2•M**$^{2+}$**•Peptide** complex.

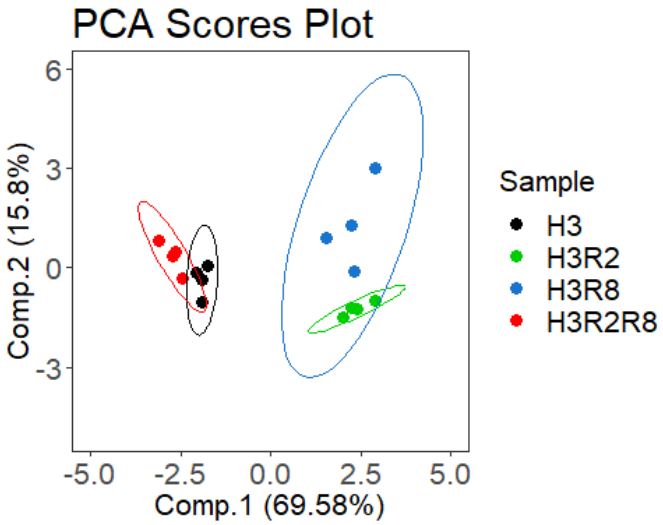

Figure S-29. PCA scores plot with 95% confidence intervals for the 7-factor **1•G2•M**$^{2+}$**•Peptide** sensor array (obtained from PCA of data in Figure S-28). [**1**] = 20 μM, [**G2**] = 1.5 μM, [Metal] = 10 μM, [Peptides] = 10 μM, [BisTris] = 20 mM (pH 5.5).

1•G3 Sensor Responses to H3 Peptides

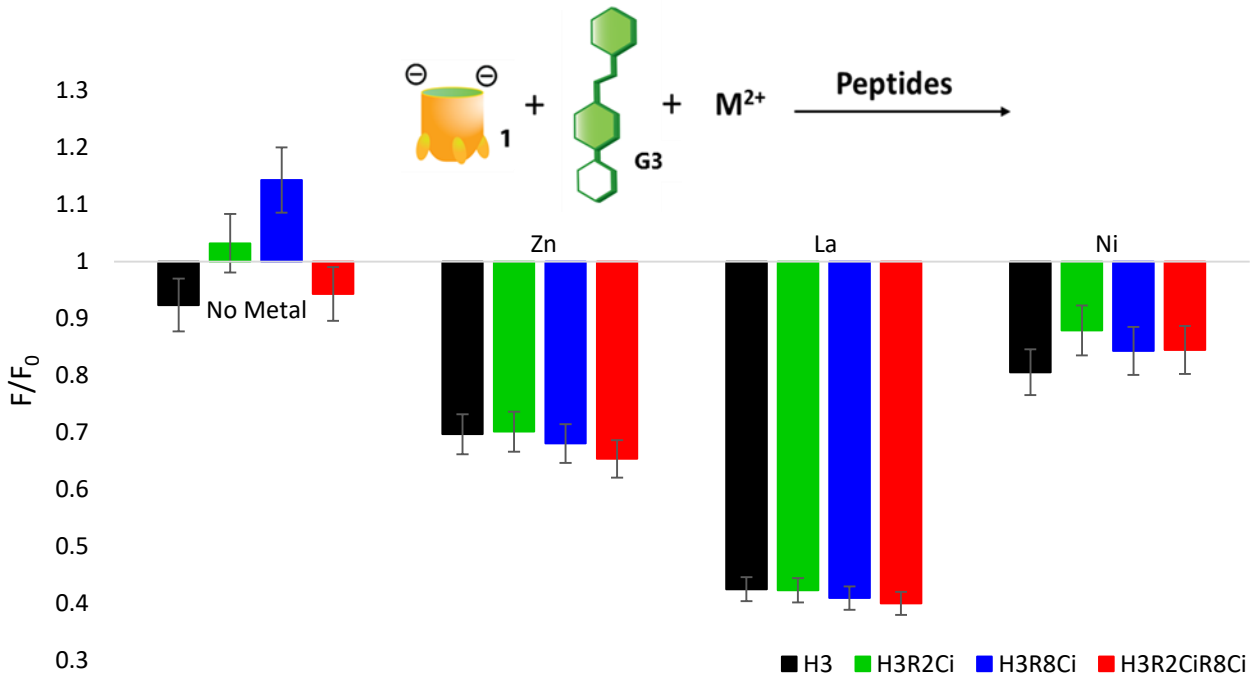

Figure S-30. Relative fluorescence responses of the **1•G3•M**$^{2+}$ complex in 20 mM Tris buffer, pH 7.4. [**1**] = 20 μM, [**G3**] = 1.5 μM, [Metal] = 10 μM, [Peptides] = 10 μM. F_0 = fluorescence response of the **1•G2•M**$^{2+}$ complex, F = fluorescence response of the **1•G3•M**$^{2+}$**•Peptide** complex.

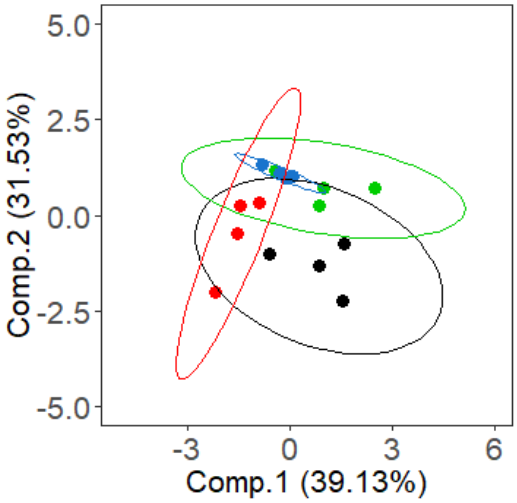

Figure S-31. PCA scores plot with 95% confidence intervals for the 4-factor **1•G3•M**$^{2+}$**•Peptide** sensor array (obtained from PCA of data in Figure S-30). [**1**] = 20 μM, [**G3**] = 1.5 μM, [Metal] = 10 μM, [Peptides] = 10 μM, [Tris] = 20 mM (pH 7.4).

2•G2 Sensor Responses to H3 Peptides

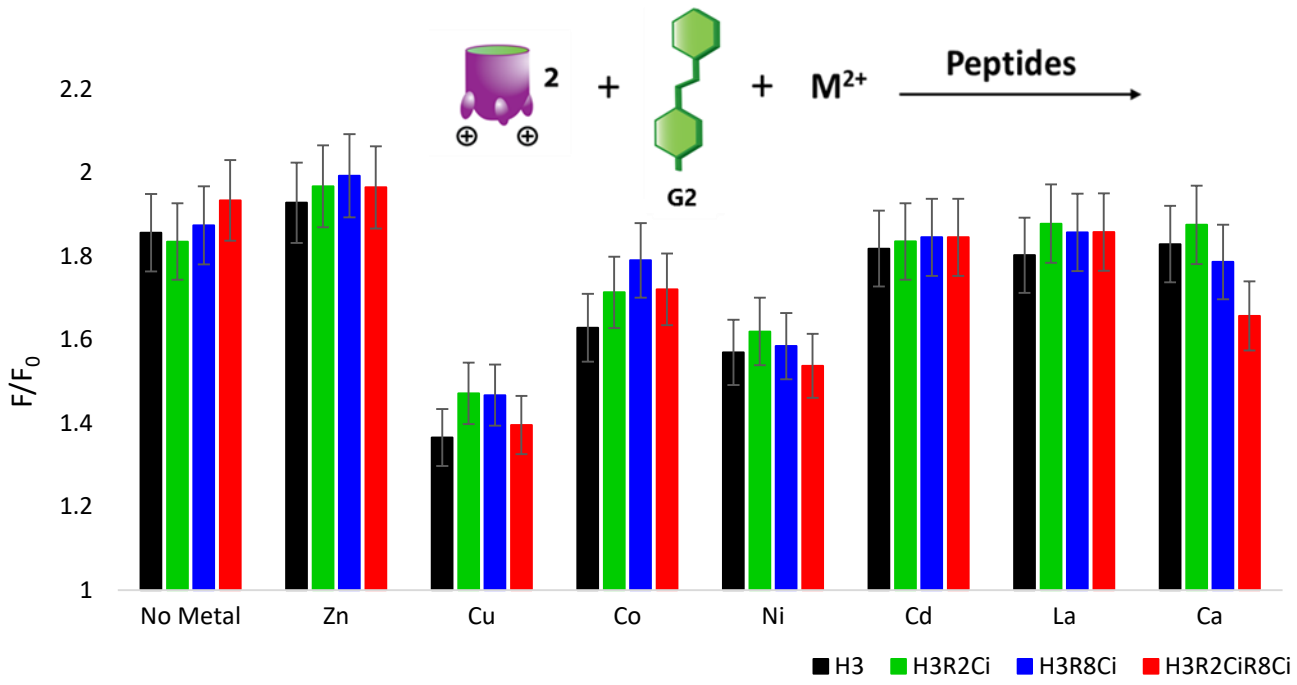

Figure S-32. Relative fluorescence responses of the **2•G2•M**$^{2+}$ complex in 20 mM Tris buffer, pH 7.4. [**2**] = 20μM, [**G2**] = 1.5 μM, [Metal] = 10 μM, [Peptides] = 10 μM. F_0 = fluorescence response of the **2•G2•M**$^{2+}$ complex, F = fluorescence response of the **2•G2•M**$^{2+}$**•Peptide** complex.

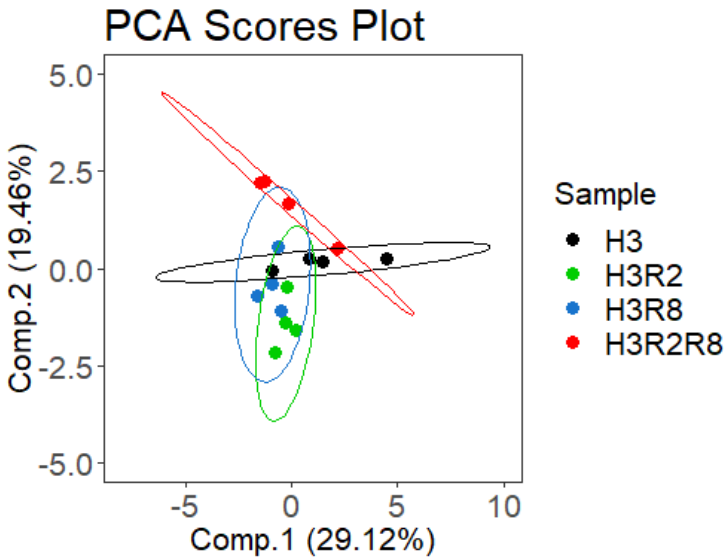

Figure S-33. PCA scores plot with 95% confidence intervals for the 4-factor **2•G2•M**$^{2+}$**•Peptide** sensor array (obtained from PCA of data in Figure S-32). [**2**] = 20 μM, [**G2**] = 1.5 μM, [Metal] = 10 μM, [Peptides] = 10 μM, [Tris] = 20 mM (pH 7.4).

5. Principal Component Analysis

1•G2 Sensor – Single pH

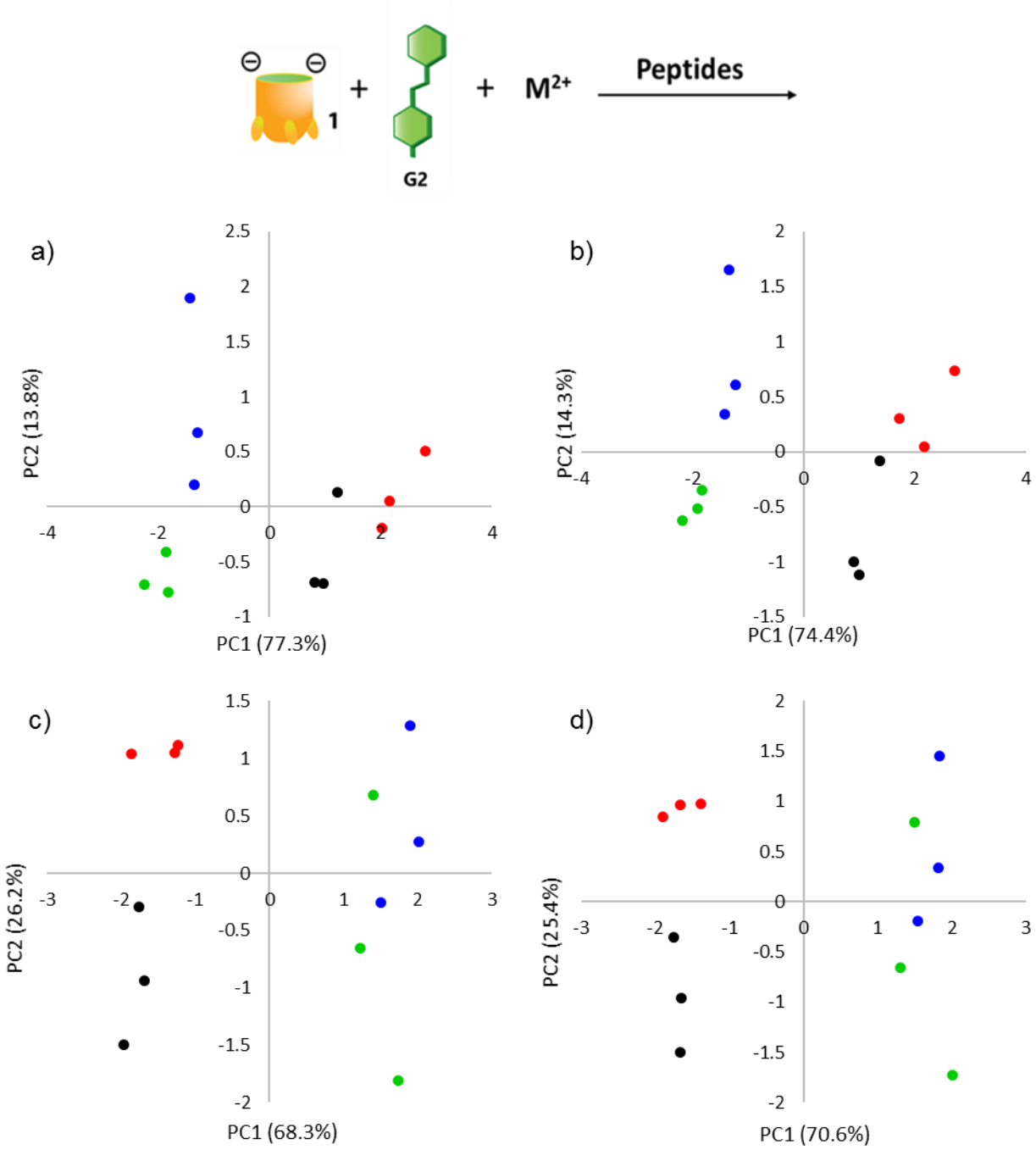

Figure S-34. PCA scores plots for various minimized 4-factor **1•G2•M^{2+}•Peptide** sensor arrays using different combinations of metal cofactors. a) No Metal, Zn^{2+}, Ni^{2+}, and La^{2+} at pH 5.5. b) No Metal, Zn^{2+}, Co^{2+}, and La^{2+} at pH 5.5. c) No Metal, Zn^{2+}, Ni^{2+}, and La^{2+} at pH 7.4. d) No Metal, Zn^{2+}, Co^{2+}, and La^{2+} at pH 7.4. [**1**] = 20 μM, [**G2**] = 1.5 μM, [Metal] = 10 μM, [Peptides] = 10 μM, [Tris] = 20 mM (pH 7.4), [BisTris] = 20 mM (pH 5.5).

1•G2 Sensor – Dual pH

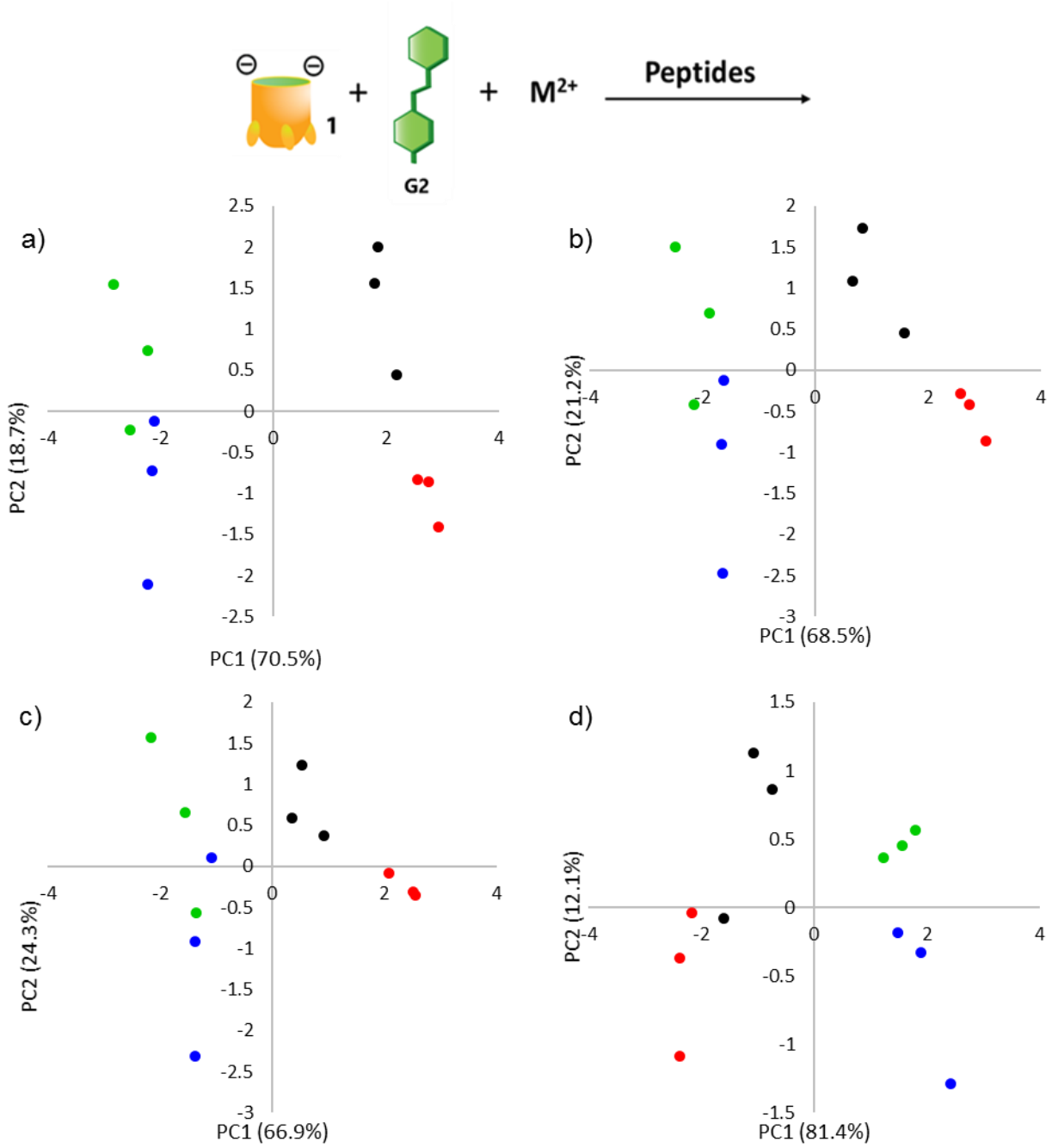

Figure S-35. PCA scores plots for various minimized dual-pH **1•G2•M^{2+}•Peptide** sensor arrays using different combinations of metal cofactors. a) 8-factor array (No Metal, Zn^{2+}, Co^{2+}, and La^{2+} at pH 5.5 and 7.4). b) 6-factor array (No Metal, Zn^{2+}, and La^{2+} at pH 5.5 and 7.4). c) 4-factor array (No Metal and Zn^{2+} at pH 5.5 and 7.4). d) 4-factor array (No Metal and La^{2+} at pH 5.5 and 7.4). [**1**] = 20 μM, [**G2**] = 1.5 μM, [Metal] = 10 μM, [Peptides] = 10 μM, [Tris] = 20 mM (pH 7.4), [BisTris] = 20 mM (pH 5.5).

1•G1 Sensor – Single pH

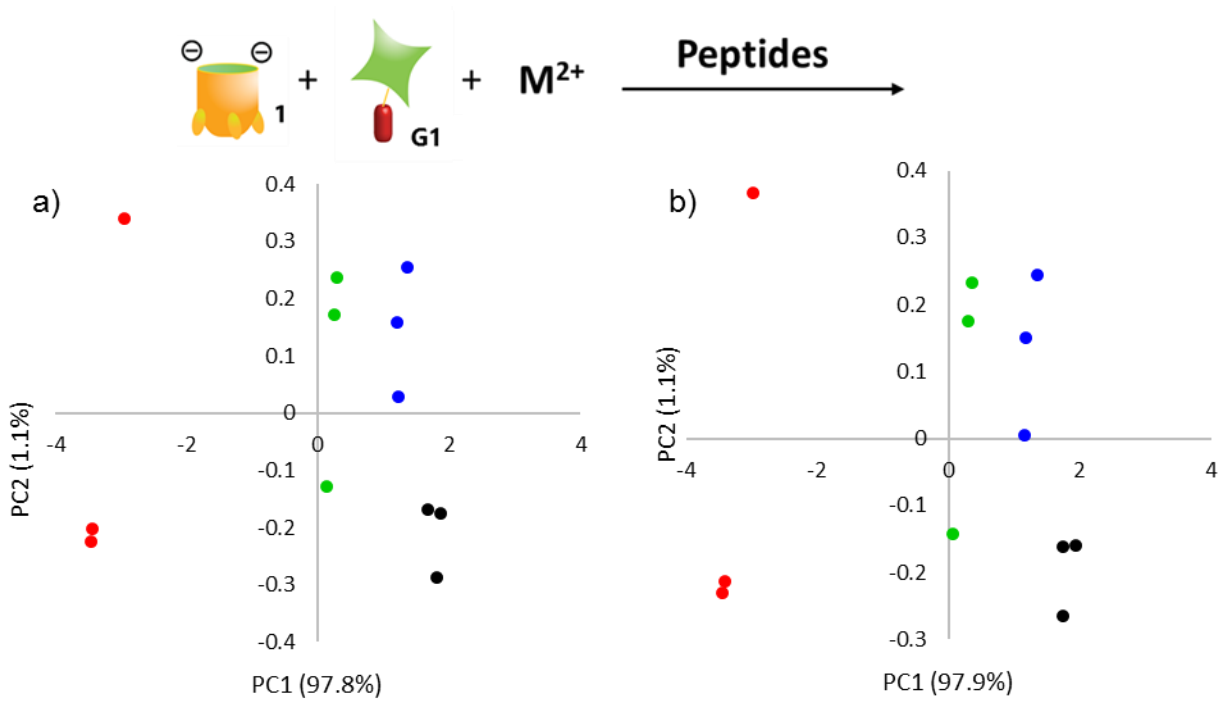

Figure S-36. PCA scores plots for various minimized 4-factor **1•G1•M^{2+}•Peptide** sensor arrays using different combinations of metal cofactors. a) No Metal, Zn^{2+}, Ni^{2+}, and La^{2+} at pH 7.4. b) No Metal, Zn^{2+}, Co^{2+}, and La^{2+} at pH 7.4. [**1**] = 20 μM, [**G1**] = 3.0 μM, [Metal] = 10 μM, [Peptides] = 10 μM, [Tris] = 20 mM (pH 7.4).

1•G1 and 1•G2 Dual Fluorophore Sensor – Single pH

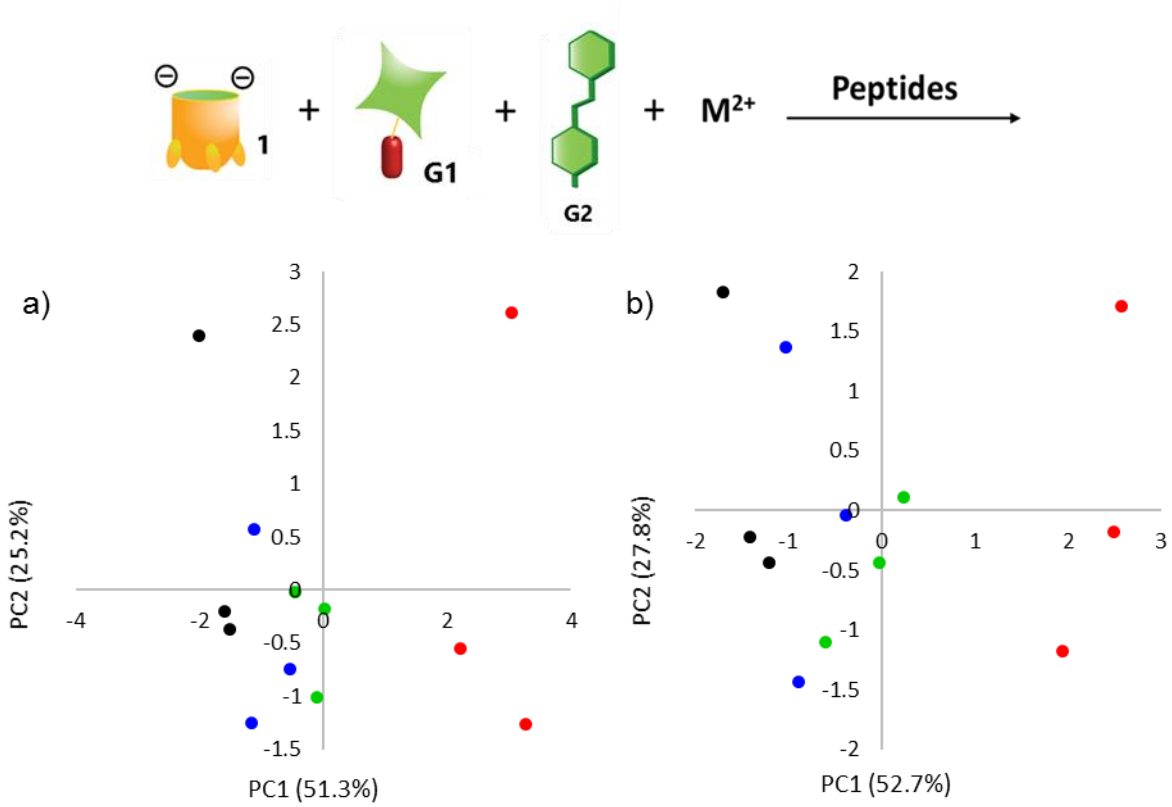

Figure S-37. PCA scores plots for various combined **1•G2•M^{2+}•Peptide** and **1•G1•M^{2+}•Peptide** sensor arrays using different combinations of metal cofactors. a) 6-factor array (No Metal, Zn^{2+}, and La^{2+} at pH 7.4). b) 4-factor array (No Metal and La^{2+} at pH 7.4). [**1**] = 20 μM, [**G1**] = 3.0 μM, [**G2**] = 1.5 μM, [Metal] = 10 μM, [Peptides] = 10 μM, [Tris] = 20 mM (pH 7.4).

6. References

1. S. M. Biros, E. C. Ullrich, F. Hof, L. Trembleau and J. Rebek, Jr. *J. Am. Chem. Soc.* 2004, **126**, 2870.
2. Y. Liu, L. Perez, M. Mettry, C. J. Easley, R. J. Hooley and W. Zhong, *J. Am. Chem. Soc.* 2016, **138**, 10746.
3. Y. Liu, M. Mettry, A. D. Gill, L. Perez, W. Zhong and R. J. Hooley, *Anal. Chem.* 2017, **89**, 11113.
4. Y. Liu, J. Lee, L. Perez, A. D. Gill, R. J. Hooley and W. Zhong, *J. Am. Chem. Soc.* 2018, **140**, 13869.
5. S. Mosca, Y. Yang and J. Rebek, Jr. *Nat. Proc.* 2016, **11**, 1371.